Supporting Information

Capsoplexes: Encapsulating complexes via guest recognition

Philipp J. Altmann and Alexander Pöthig*

Catalysis Research Center & Department of Chemistry, Technische Universität München, Ernst-Otto-Fischer-Str. 1, 85747 Garching bei München, Germany

1. General remarks

Chemicals were purchased from commercial suppliers and used without further purification if not stated otherwise. Anhydrous acetonitrile was obtained from an MBraun solvent purification system, degassed by freeze-pump-thaw technique and stored over 3 Å molecular sieves. Caesium carbonate was dried by heating a sample in vacuo at 120 °C for 48 hours.

Liquid NMR spectra were recorded on a Bruker Avance DPX 400 and a Bruker DRX 400. Chemical shifts are given in parts per million (ppm) and the spectra were referenced by using the residual solvent shift as internal standards (dimethyl sulfoxide-d_6, ^{1}H NMR δ 2.50, ^{13}C NMR δ 39.52; acetonitrile-d_3, ^{1}H NMR δ 1.94, ^{13}C NMR δ 118.26). MS-ESI analyses were performed on a Thermo Scientific LCQ/Fleet spectrometer by Thermo Fisher Scientific. Elemental analyses were obtained from the microanalytical laboratory of the Technical University of Munich.

2. Experimental details

Ethylene-bis(trifluoromethane-sulfonate), 3,5-bis(imidazol-1-ylmethyl)-1-(tetrahydropyran-2-yl)-1*H*-pyrazole (**1**) and $\mathbf{Ni_2L^{Me}(PF_6)_2}$ were synthesised according to literature procedures.[1,2]

Ethylene-bridged calix[4]imidazolium[2]pyrazole tetrakis(hexafluorophosphate) ($\mathbf{H_6L^{Et}(PF_6)_4}$ · MeCN)

Under inert atmosphere a 1 L Schlenk flask was charged with **1** (891 mg, 2.85 mmol, 1 equiv.) and 500 mL dry acetonitrile were added. The clear solution was cooled to -40 °C and subsequently a solution of ethylene-bis(trifluoromethane-sulfonate) (930 mg, 2.85 mmol, 1 equiv.) in 50 mL dry acetonitrile was added with vigorous stirring over the course of 45 min. The resulting mixture was allowed to warm to room temperature overnight with stirring and the solvent was then removed in vacuo. The residue was redissolved in 30 mL ethanol and filtered. The filtrate was treated with 1.5 mL of a 1:1 mixture of trifluoromethanesulfonic anhydride and water and stirred at room temperature for 4 h. Diethyl ether (150 mL) was added to precipitate a white solid that was washed with diethyl ether (2x 20 mL) and acetone (2x 20 mL). The resulting white solid was dissolved in 4 mL water and NH_4OH(aq) (25 %, 1 mL) was added at room temperature. The mixture was stirred for 15 min at room temperature and subsequently added to a solution of NH_4PF_6 (1.16 g, 7.13 mmol, 2.5 equiv.) in 5 mL water. The resulting suspension was stirred at room temperature for 30 min and filtered. The residue was washed with water (2x 10 mL), redissolved in a minimum of acetonitrile and precipitated with diethyl ether. After washing with diethyl ether (2x 10 mL) and drying in vacuo, $\mathbf{H_6L^{Et}(PF_6)_4}$ · **MeCN** was obtained as a white solid in a yield of 669 mg (0.59 mmol, 41 %). One equivalent of MeCN was found to remain in the sample. ^{1}H NMR (400 MHz, DMSO-d_6, 298 K): δ (ppm) = 13.15 (br s, 2H, H_{NH}), 8.89 (s, 4H, H_{NCHN}), 7.64 (*virt.* s, 8H, H_{NCHC}), 6.03 (s, 2H, H_{CCHC}), 5.39 (s, 8H, H_{CH2}), 4.73 (s, 8H, H_{CH2}), 2.07 (s, 3H, H_{MeCN}). ^{13}C{^{1}H} NMR (101 MHz, DMSO-d_6, 298 K): δ (ppm) = 144.0 (br), 136.6, 123.2, 122.7, 118.1 (MeCN), 104.3, 48.8, 44.7 (br), 1.1 (MeCN). ^{31}P NMR (161.98 MHz, DMSO-d_6, 298 K): δ (ppm) = -144.2. Elemental analysis (%) calcd for $\mathbf{H_6L^{Et}(PF_6)_4}$ · **MeCN**: C 29.67, H 3.11, N 16.06; found: C 29.90, H 3.18, N 15.67. ESI-MS (m/z): 219.09 ($\mathbf{H_6L^{Et}}$ -3PF_6^-)$^{3+}$, 328.17 ($\mathbf{H_6L^{Et}}$ -H^+-3PF_6^-)$^{2+}$, 401.15 ($\mathbf{H_6L^{Et}}$ -2PF_6^-)$^{2+}$, 801.01 ($\mathbf{H_6L^{Et}}$ -H^+-2PF_6^-)$^+$, 947.02 ($\mathbf{H_6L^{Et}}$ -3PF_6^-)$^+$.

Ethylene-bridged (calix[4]imidazolylidene[2]pyrazolato)dinickel(II) bis(hexafluorophosphate) ($\mathbf{Ni_2L^{Et}(PF_6)_2}$)

To a mixture of $\mathbf{H_6L^{Et}(PF_6)_4}$ · **MeCN** (100 mg, 0.088 mmol, 1 equiv.), anhydrous nickel acetate (31 mg, 0.177 mmol, 2 equiv.) and caesium carbonate (287 mg, 0.880 mmol, 10 equiv.) 5 mL dry acetonitrile were added under inert atmosphere and the resulting mixture was stirred at 70 °C for 16 h. The suspension was allowed to cool to room temperature and was concentrated to approximately 2 mL. Subsequently, 10 mL of diethyl ether were added to precipitate a yellow solid which was isolated by centrifugation and washed with water (3x 10 mL). The residue was dissolved in 2 mL acetonitrile, filtered and 10 mL diethyl ether were added to the solution to precipitate a solid that was washed with diethyl ether (3x 10 mL). The crude product was purified by fractional precipitation (MeCN, Et_2O). After drying in vacuo, $\mathbf{Ni_2L^{Et}(PF_6)_2}$ was obtained as pale yellow solid in a yield of 55 mg (0.060 mmol, 68 %). ^{1}H NMR (400.13 MHz, CD_3CN, 298 K): δ (ppm) = 7.23 (d, ^3J = 1.96 Hz, 4H, H_{NCHC}), 7.11 (d, ^3J = 1.94 Hz, 4H, H_{NCHC}), 6.27 (s, 2H, H_{CCHC}), 5.50 (d, ^2J = 15.47 Hz, 4H, H_{CH2}), 5.20 (m, 4H, H_{CH2}), 5.10 (d, ^2J = 15.47 Hz, 4H, H_{CH2}), 4.46 (m, 4H, H_{CH2}). ^{13}C{^{1}H} NMR (100.62 MHz, CD_3CN, 298 K): δ (ppm) = 158.6, 145.8, 124.1, 123.7, 103.5, 48.8, 47.5. ^{31}P NMR (161.98 MHz, CD_3CN, 298 K): δ (ppm) = -144.6. Elemental analysis (%) calcd for $\mathbf{Ni_2L^{Et}(PF_6)_2}$: C 34.17, H 2.87, N 18.39; found: C 34.56, H 3.06, N 18.11. ESI-MS (m/z): 311.38 ($\mathbf{Ni_2L^{Et}}$)$^{2+}$, 666.97 ($\mathbf{Ni_2L^{Et}}$ +$HCOO^-$)$^+$, 767.15 ($\mathbf{Ni_2L^{Et}}$ +PF_6^-)$^+$.

Ethylene-bridged bis[(calix[4]imidazolylidene[2]pyrazolato)bisnickel(II)] chloride tris(hexafluorophosphate) ($[(Ni_2L^{Et})_2Cl](PF_6)_3$)

To a mixture of $H_6L^{Et}(PF_6)_4 \cdot MeCN$ (150 mg, 0.132 mmol, 1 equiv.), bis(triphenylphosphine)nickel(II) chloride (176 mg, 0.264 mmol, 2 equiv.) and caesium carbonate (431 mg, 1.320 mmol, 10 equiv.) 8 mL dry acetonitrile were added under inert atmosphere and the resulting suspension was stirred at 70 °C for 16 h. The suspension was allowed to cool to room temperature and was concentrated to approximately 2 mL. Subsequently, 10 mL of water were added to precipitate a yellow solid which was isolated by centrifugation and washed with water (3x 10 mL). The residue was dissolved in 2 mL acetonitrile, filtered and 10 mL diethyl ether were added to the solution to precipitate a solid that was washed with diethyl ether (3x 10 mL). The crude product was purified by fractional precipitation (MeCN, Et_2O). After drying in vacuo, $[(Ni_2L^{Et})_2Cl](PF_6)_3$ was obtained as yellow solid in a yield of 87 mg (0.100 mmol, 76 %). ^{1}H NMR (400.13 MHz, CD_3CN, 298 K): δ (ppm) = 7.08 (s, 4H, H_{NCHC}), 6.38 (br s, 4H, H_{NCHC}), 6.23 (s, 2H, H_{CCHC}), 5.40 (d, ^2J = 15.38 Hz, 4H, H_{CH2}), 5.10 (d, ^2J = 15.38 Hz, 4H, H_{CH2}), 4.31 (br s, 4H, H_{CH2}), 2.81 (br s, 4H, H_{CH2}). ^{13}C{^{1}H} NMR (100.62 MHz, CD_3CN, 298 K): δ (ppm) = 160.4 (br), 144.3, 123.5, 122.8 (br), 102.2, 47.6, 46.9 (br). ^{31}P NMR (161.98 MHz, CD_3CN, 298 K): δ (ppm) = -144.6. Elemental analysis (%) calcd for $[(Ni_2L^{Et})_2Cl](PF_6)_3$: C 36.35, H 3.05, N 19.56; found: C 36.62, H 3.22, N 19.38. ESI-MS (m/z): 311.38 $(Ni_2L^{Et})^{2+}$, 657.22 $(Ni_2L^{Et}+Cl^-)^+$, 666.97 $(Ni_2L^{Et}+HCOO^-)^+$, 767.15 $(Ni_2L^{Et}+PF_6^-)^+$.

3. NMR spectra of compound $H_6L^{Et}(PF_6)_4 \cdot MeCN$

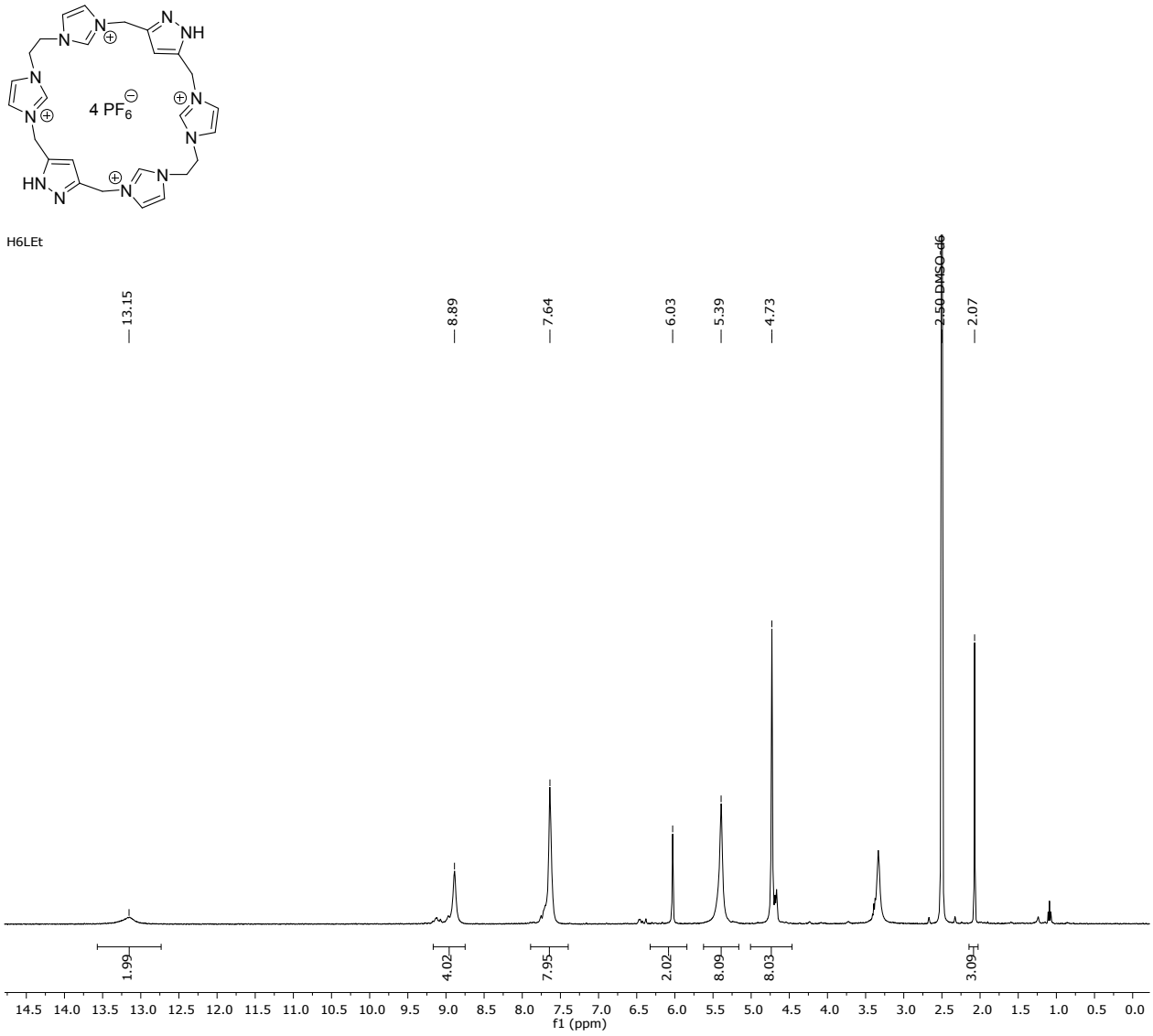

Figure S1: ^{1}H NMR spectrum of **$H_6L^{Et}(PF_6)_4 \cdot$ MeCN** in DMSO-d_6 at 400.13 MHz.

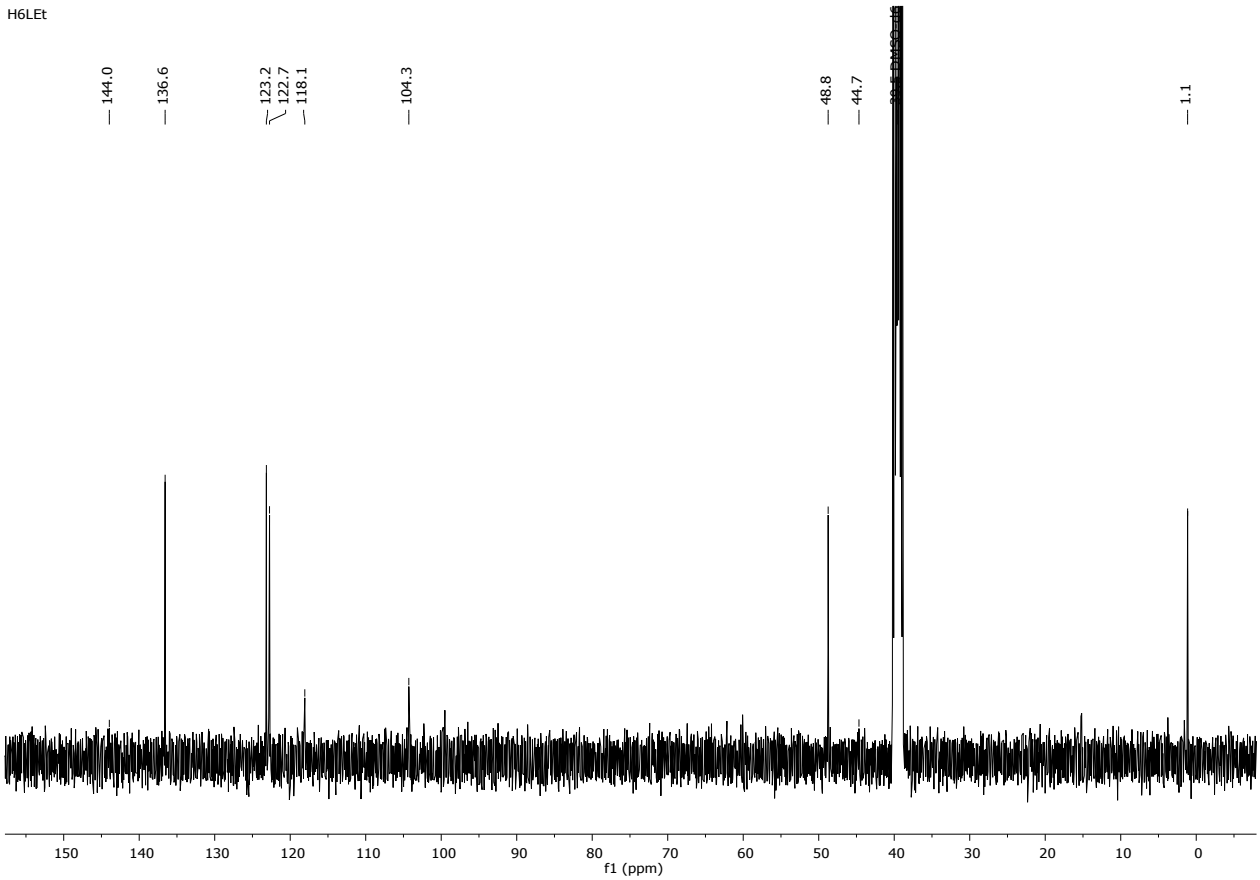

Figure S2: $^{13}C\{^{1}H\}$ NMR spectrum of $\mathbf{H_6L^{Et}(PF_6)_4}$ · **MeCN** in DMSO-d_6 at 100.62 MHz. The broad signals at 144.0 and 44.7 ppm were assigned by 2D NMR spectroscopy.

4. NMR spectra of compound $Ni_2L^{Et}(PF_6)_2$

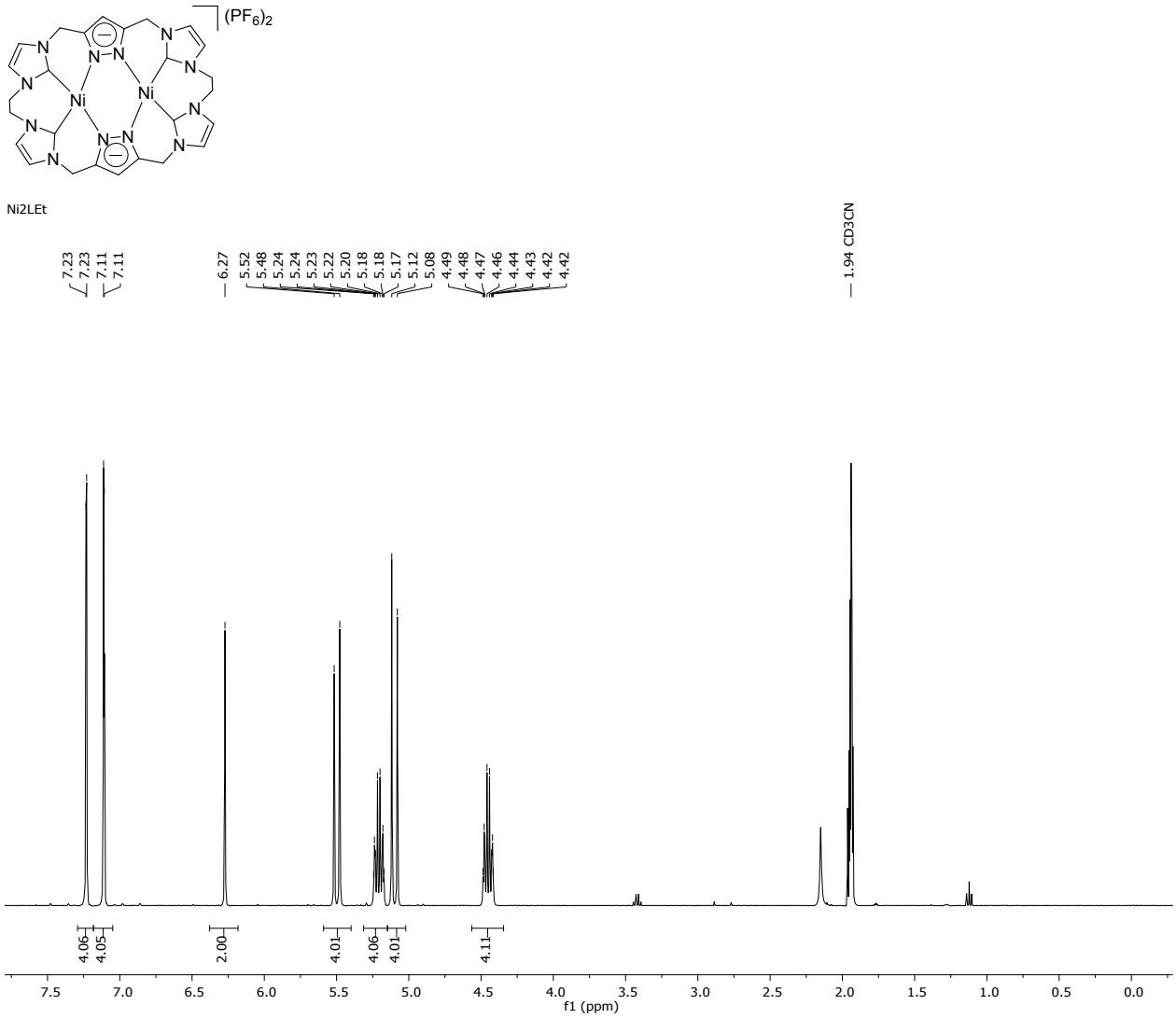

Figure S3: ^{1}H NMR spectrum of **$Ni_2L^{Et}(PF_6)_2$** in CD_3CN at 400.13 MHz.

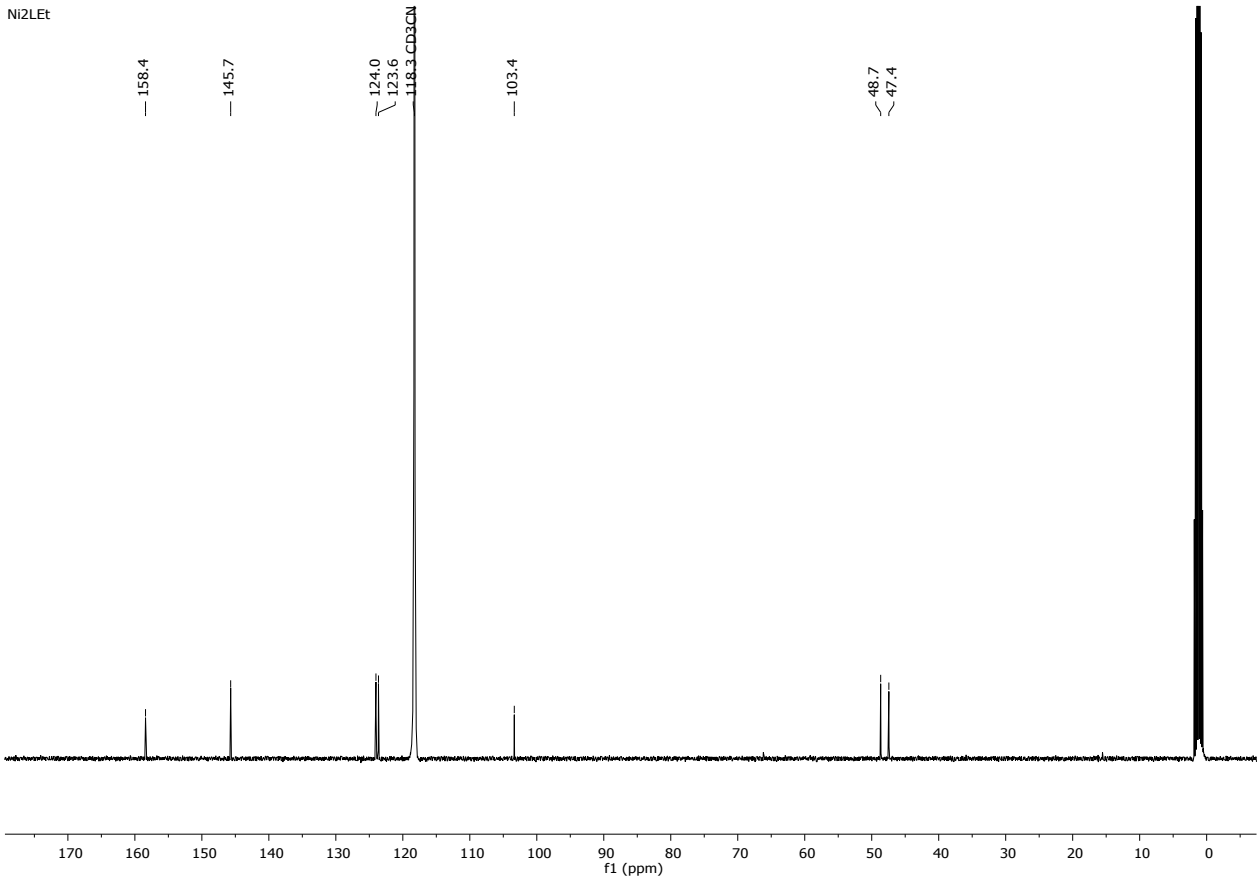

Figure S4: $^{13}C\{^{1}H\}$ NMR spectrum of $\mathbf{Ni_2L^{Et}(PF_6)_2}$ in CD_3CN at 100.62 MHz.

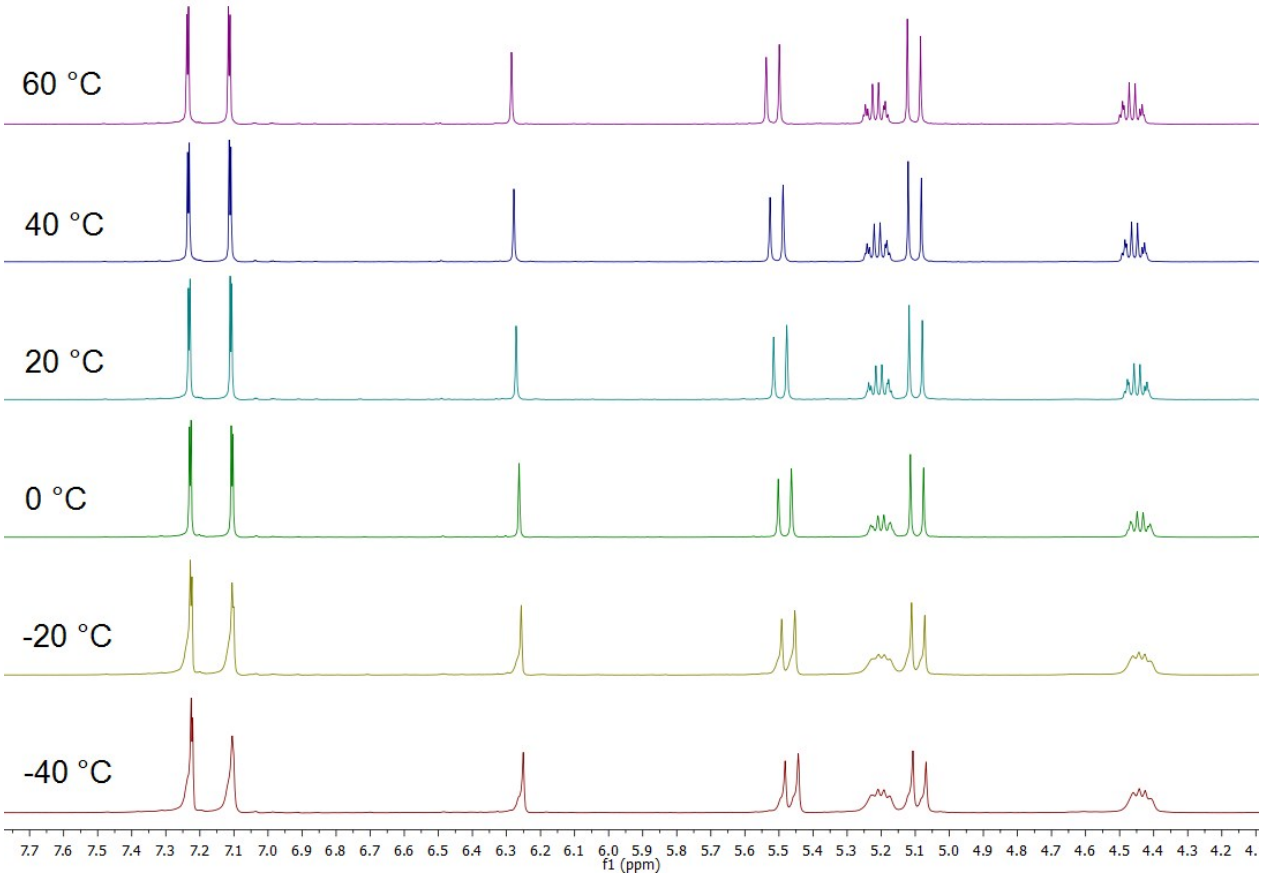

Figure S5: ^{1}H VT-NMR spectrum of **$Ni_2L^{Et}(PF_6)_2$** in CD_3CN at 400.13 MHz.

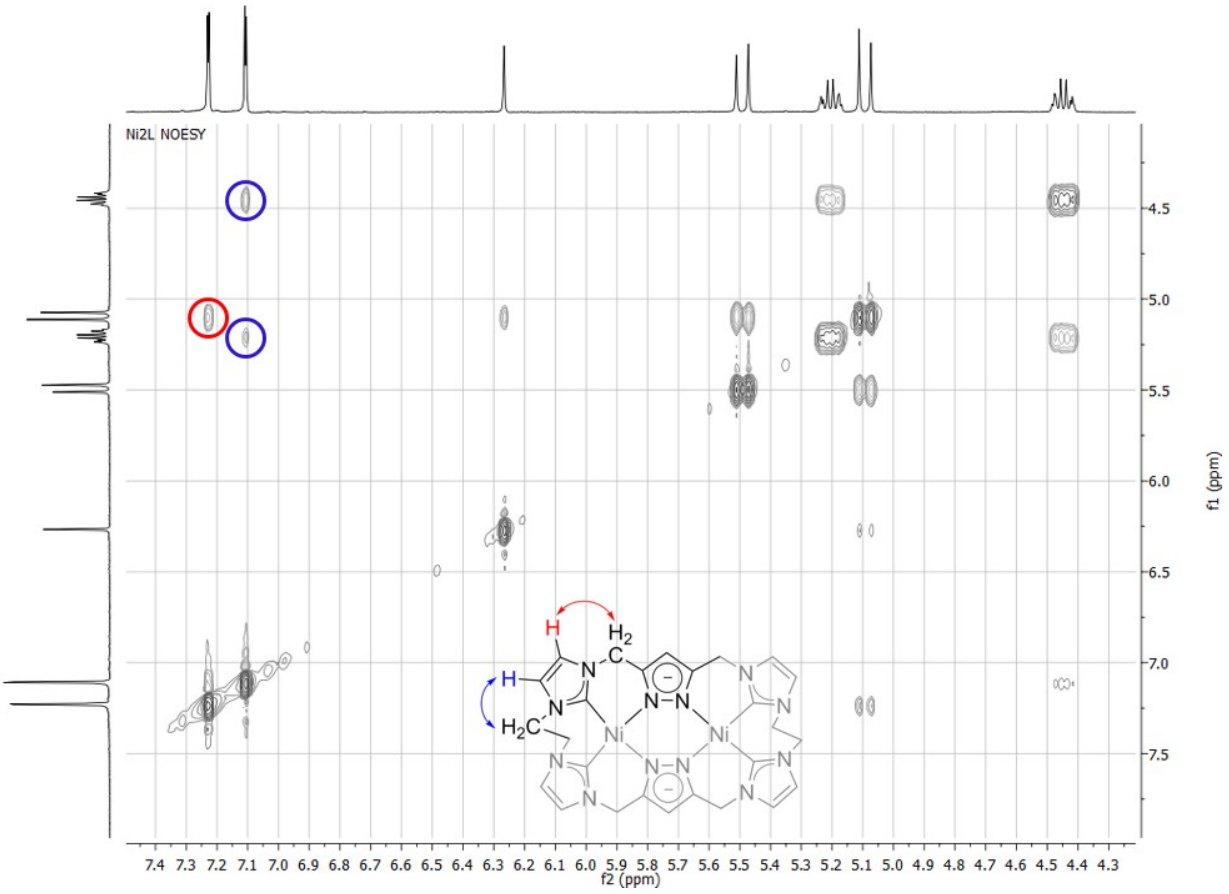

Figure S6: 2D ^{1}H -^{1}H NOESY NMR spectrum of **$Ni_2L^{Et}(PF_6)_2$** in CD_3CN at 400.13 MHz allowing for the assignment of the protons of the imidazolylidene backbone.

5. NMR spectra of compound $[(Ni_2L^{Et})_2Cl](PF_6)_3$

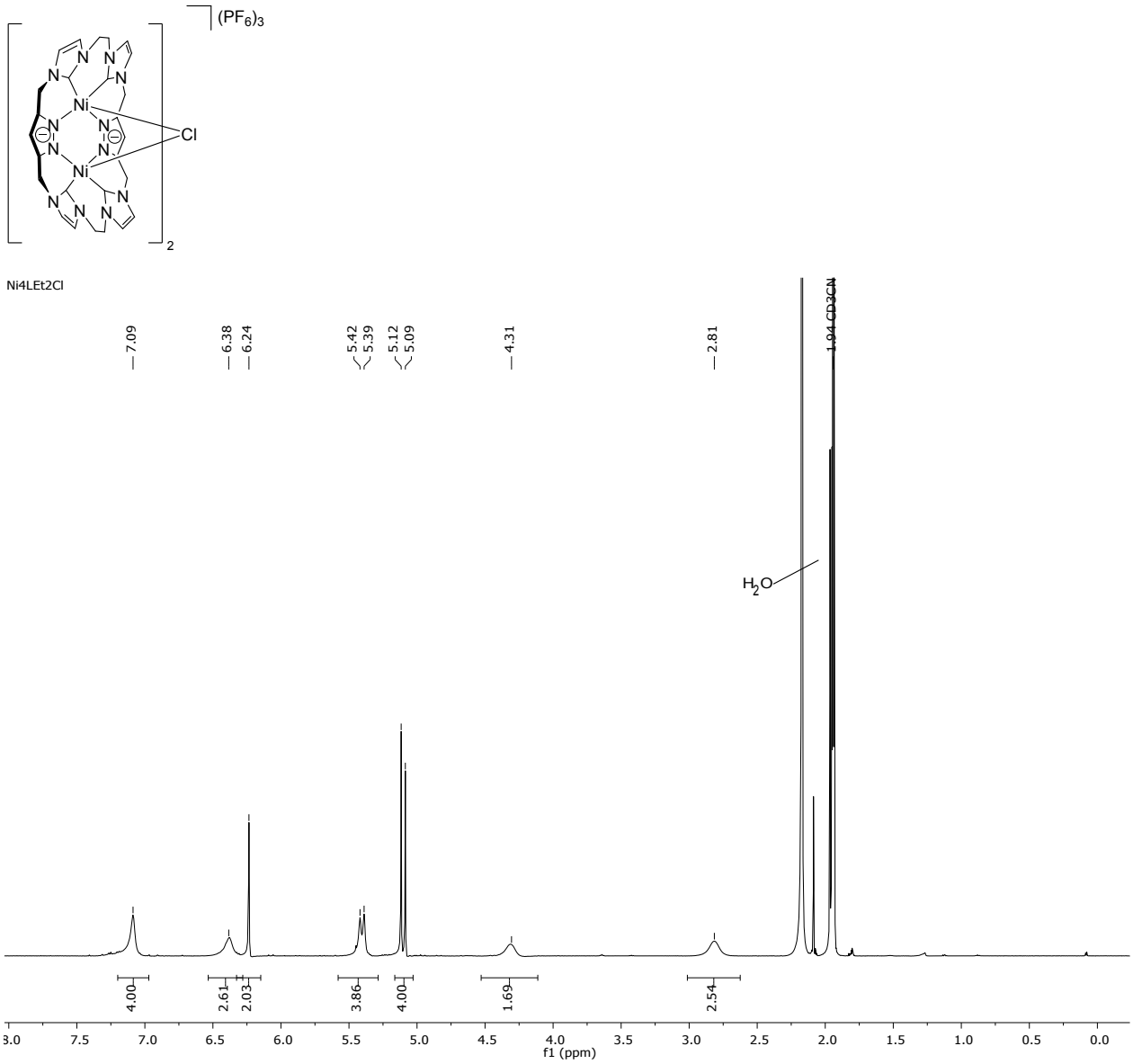

Figure S7: ^{1}H NMR spectrum of **$[(Ni_2L^{Et})_2Cl](PF_6)_3$** in CD_3CN at 400.13 MHz.

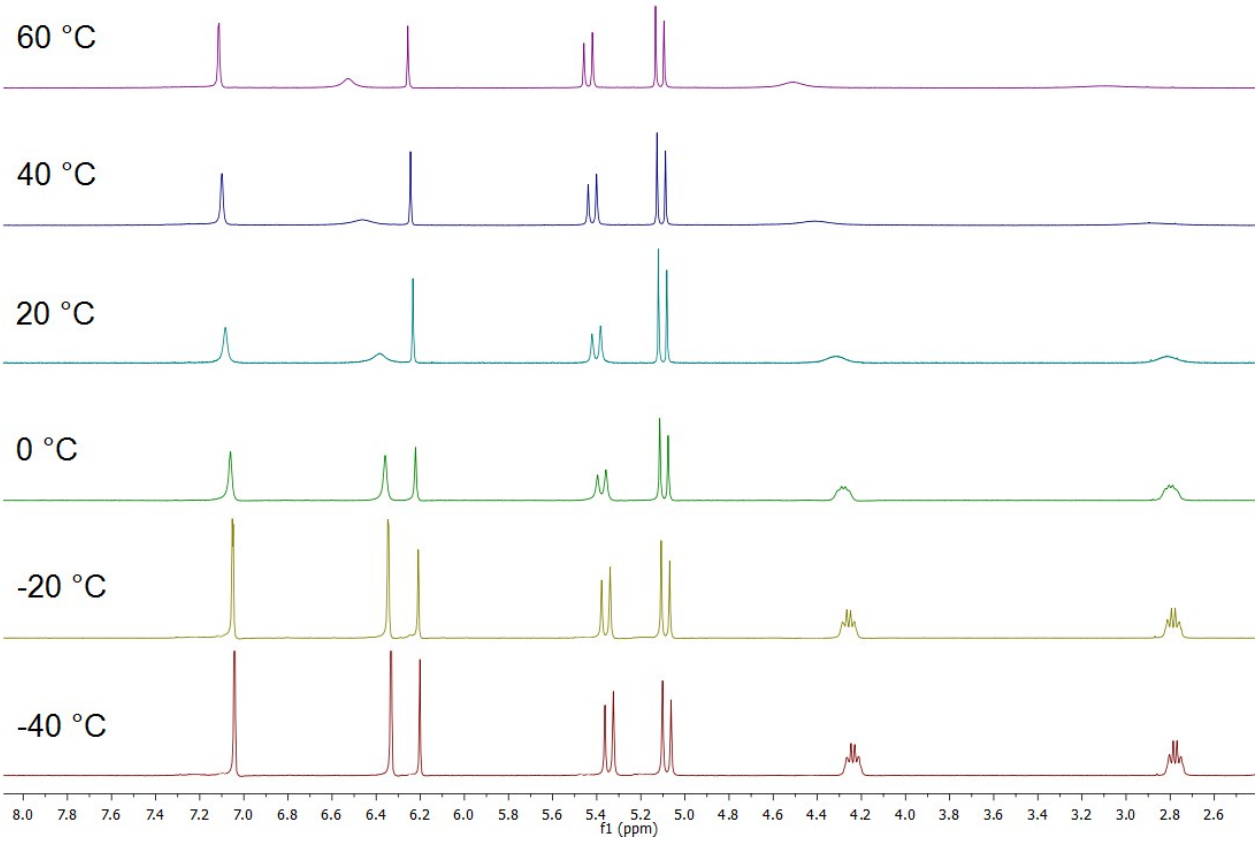

Figure S8: ^{1}H VT-NMR spectrum of **[(Ni$_2$L^{Et})$_2$Cl](PF$_6$)$_3$** in CD_3CN at 400.13 MHz.

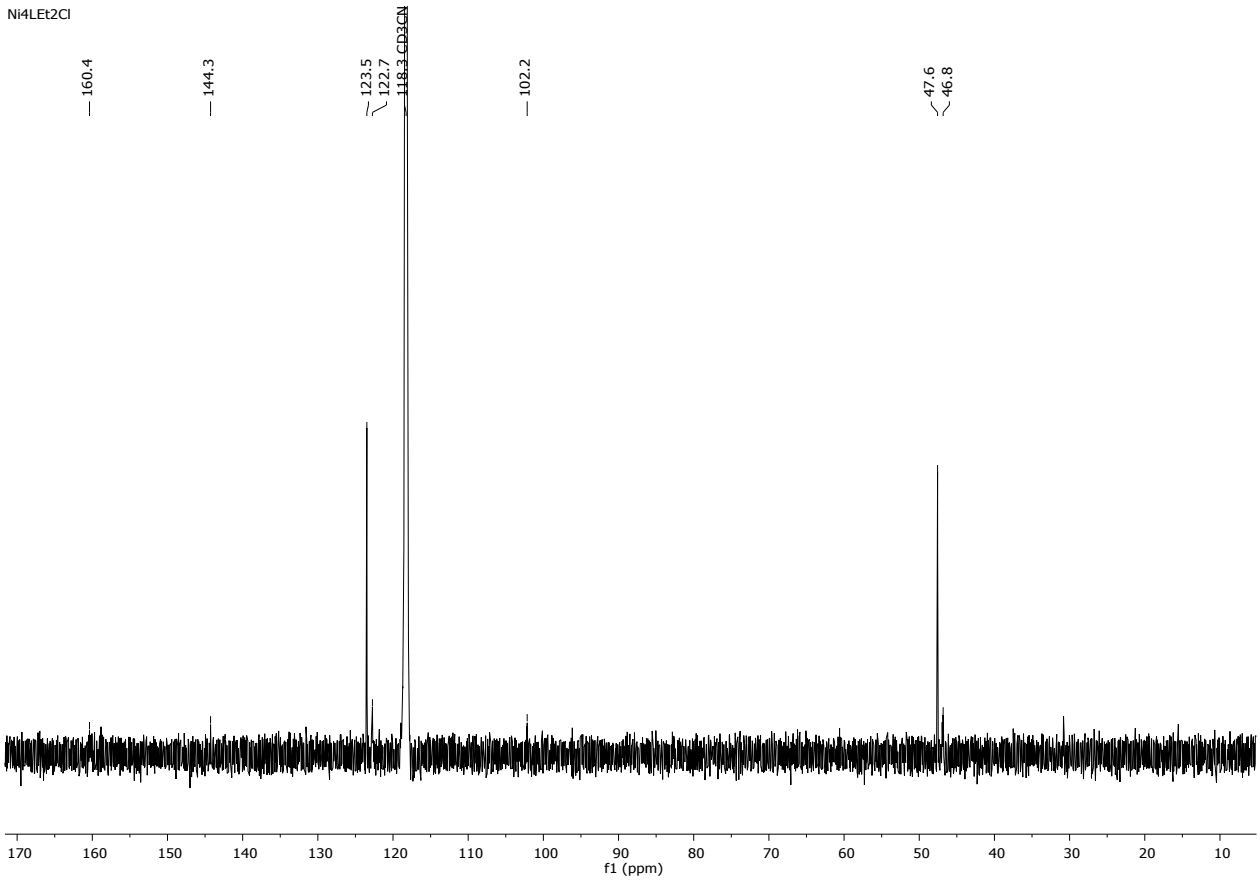

Figure S9: $^{13}C\{^{1}H\}$ NMR spectrum of **$[(Ni_2L^{Et})_2Cl](PF_6)_3$** in CD_3CN at 100.62 MHz. The broad signal at 160.4 ppm was assigned by 2D NMR spectroscopy.

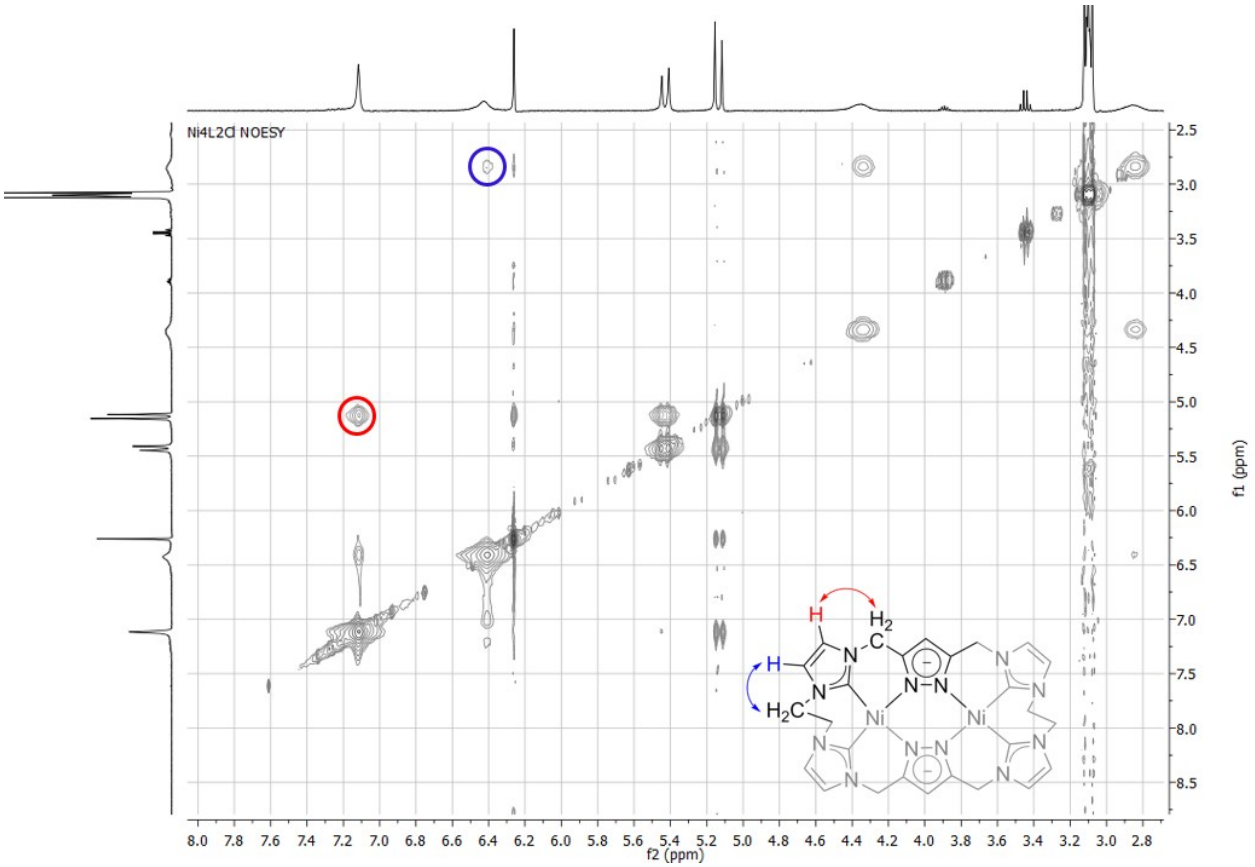

Figure S10: 2D ^{1}H -^{1}H NOESY NMR spectrum of **$[(Ni_2L^{Et})_2Cl](PF_6)_3$** in CD_3CN at 400.13 MHz allowing for the assignment of the protons of the imidazolylidene backbone.

6. NMR spectra of compound $[(Ni_2L^{Et})_2Br](PF_6)_3$ (not isolated)

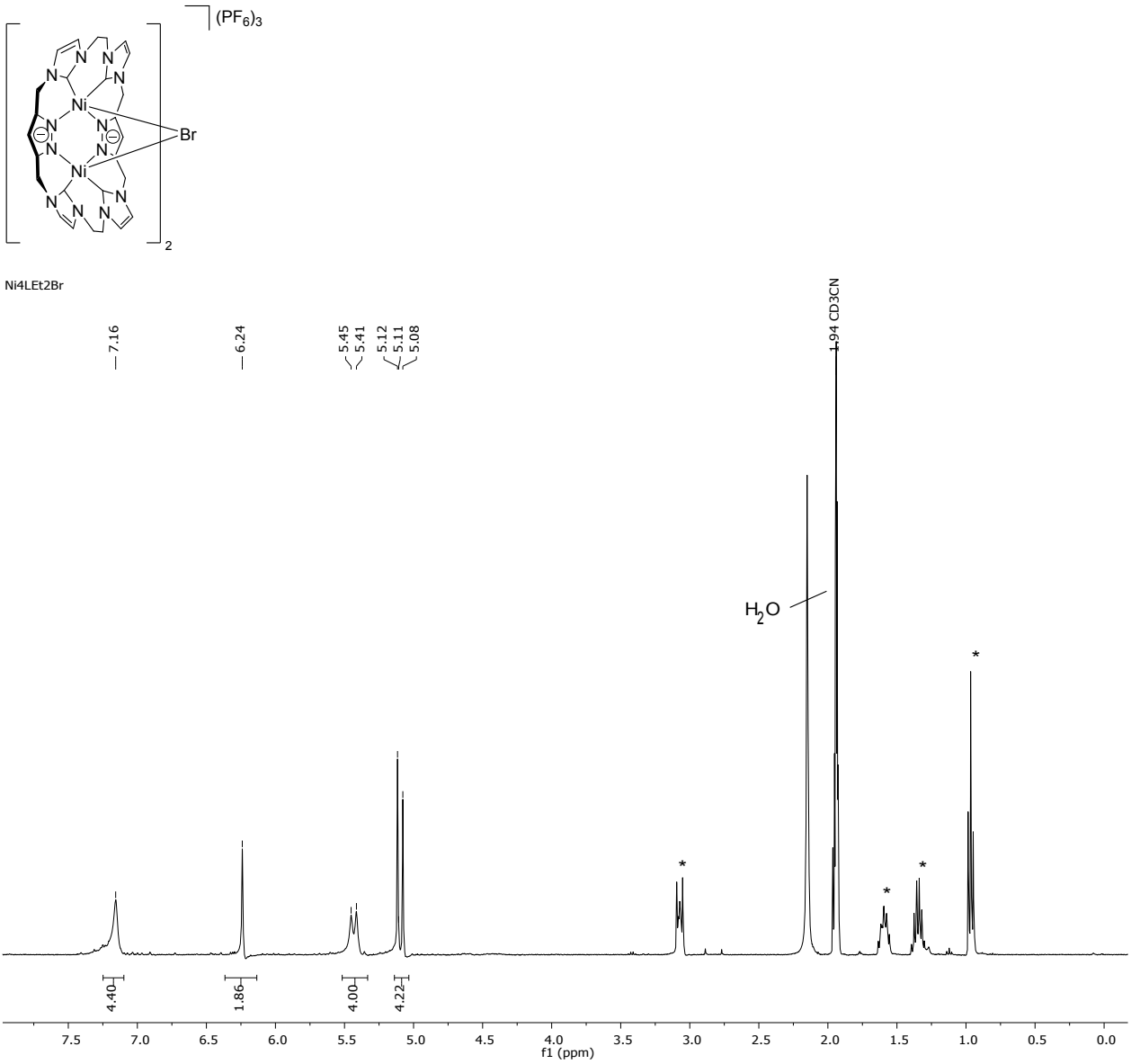

Figure S11: ^{1}H NMR spectrum of $[(Ni_2L^{Et})_2Br](PF_6)_3$ in CD_3CN at 400.13 MHz after the addition of 1 equiv. of NBu_4Br to $Ni_2L^{Et}(PF_6)_2$. The signals marked by * belong to $^+NBu_4$.

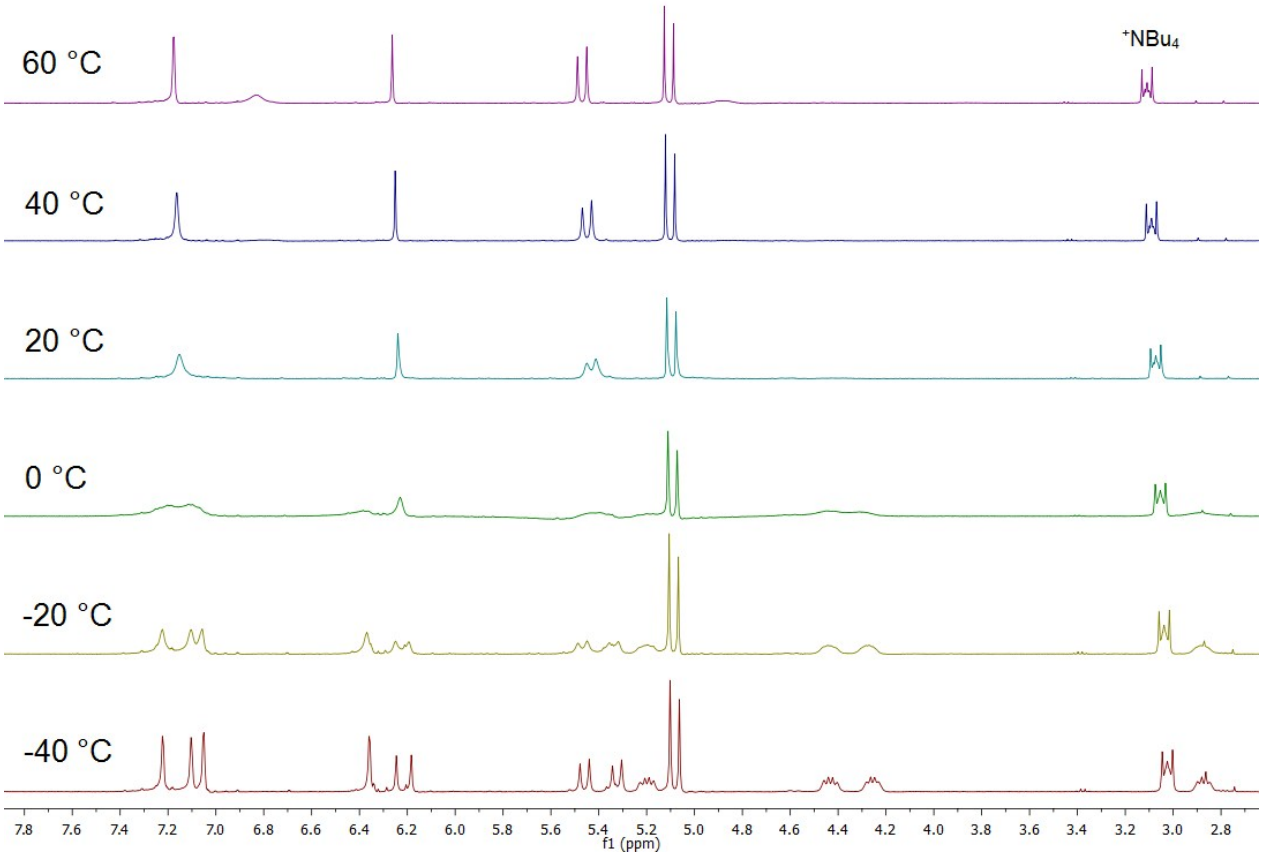

Figure S12: ^{1}H VT-NMR spectrum of **[(Ni$_2$L^{Et})$_2$Br](PF$_6$)$_3$** in CD_3CN at 400.13 MHz.

7. NMR spectra of halide titrations

7.1 Titration of NBu_4F to **$Ni_2L^{Et}(PF_6)_2$**

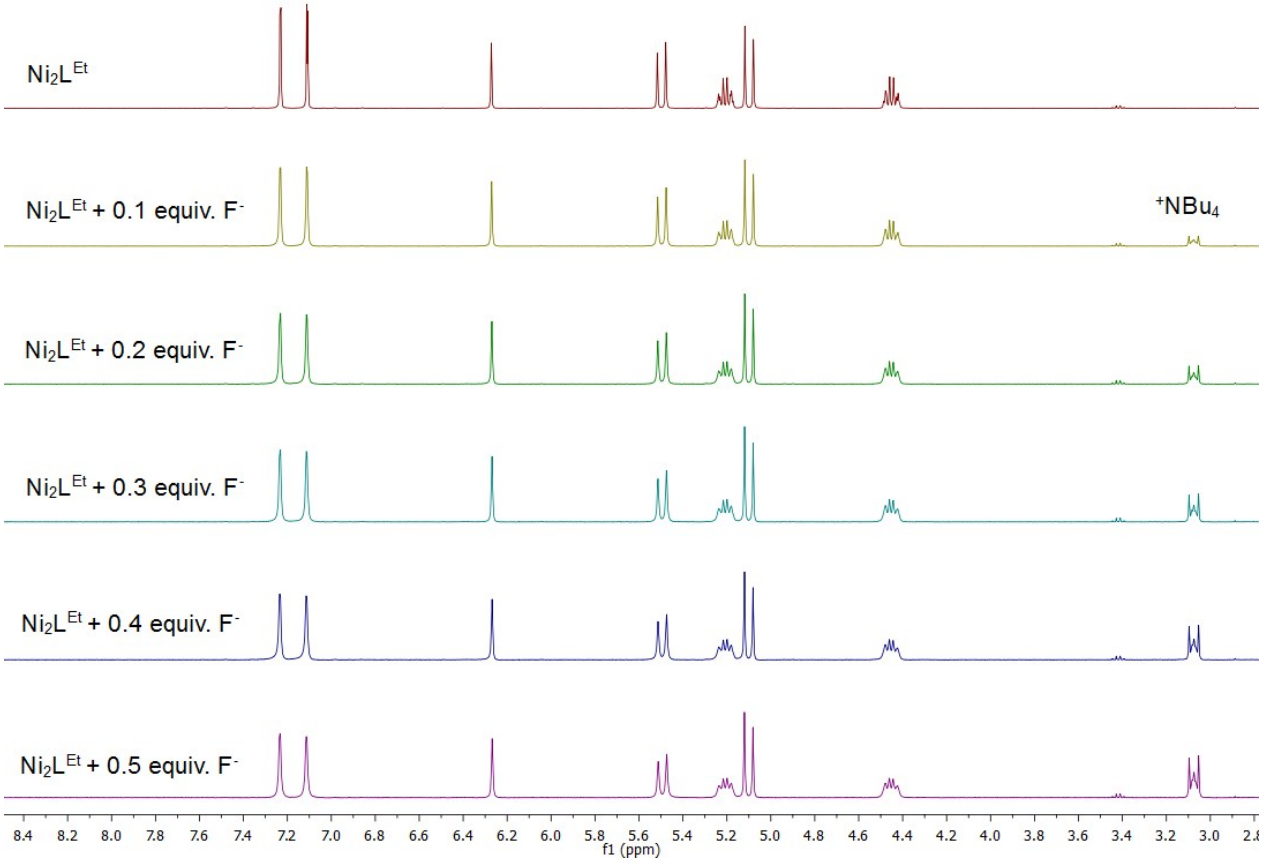

Figure S13: Stacked ^1H NMR spectra of the titration of a solution of NBu_4F in CD_3CN to a solution of **$Ni_2L^{Et}(PF_6)_2$** in CD_3CN at 400.13 MHz.

7.2 Titration of NBu_4Cl to **$Ni_2L^{Et}(PF_6)_2$**

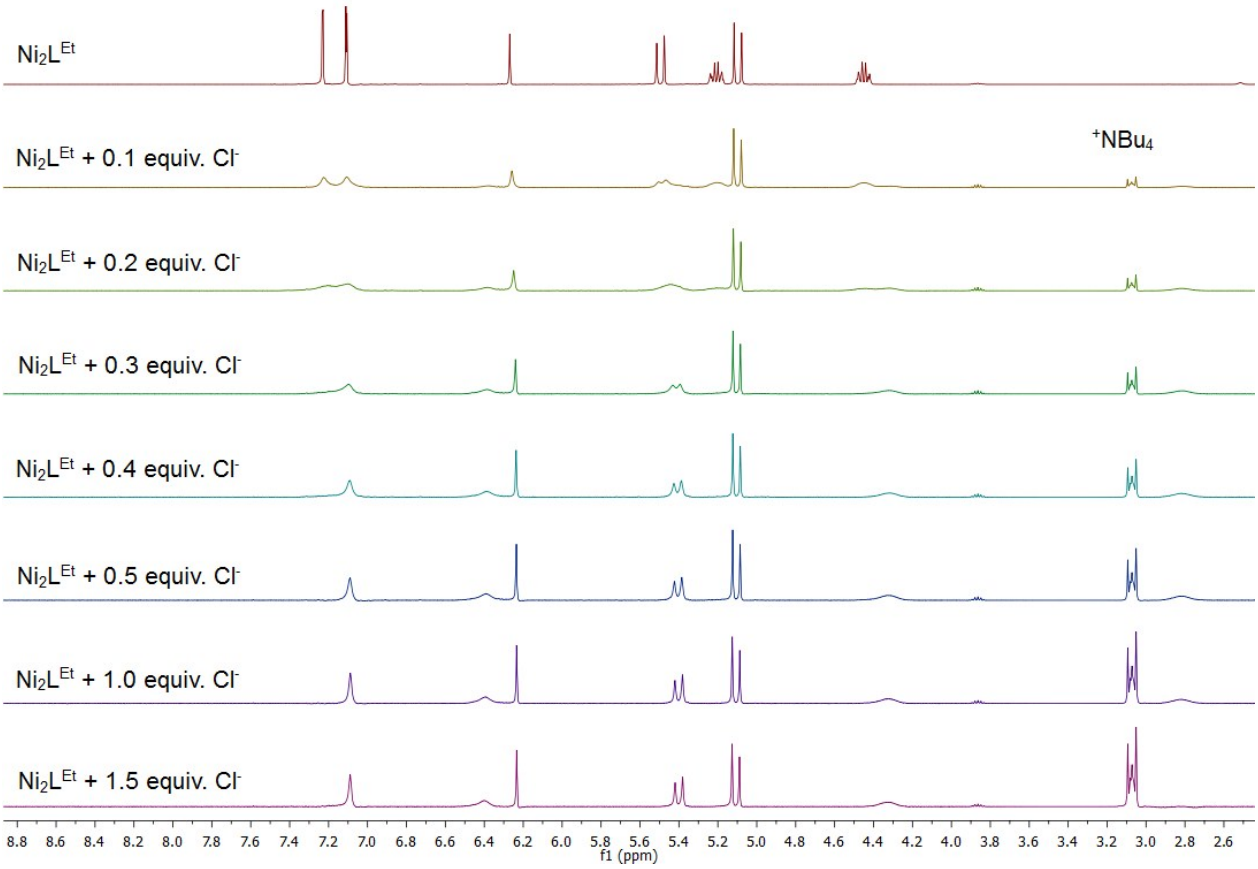

Figure S14: Stacked ^1H NMR spectra of the titration of a solution of NBu_4Cl in CD_3CN to a solution of **$Ni_2L^{Et}(PF_6)_2$** in CD_3CN at 400.13 MHz.

7.3 Titration of NBu_4Br to **$Ni_2L^{Et}(PF_6)_2$**

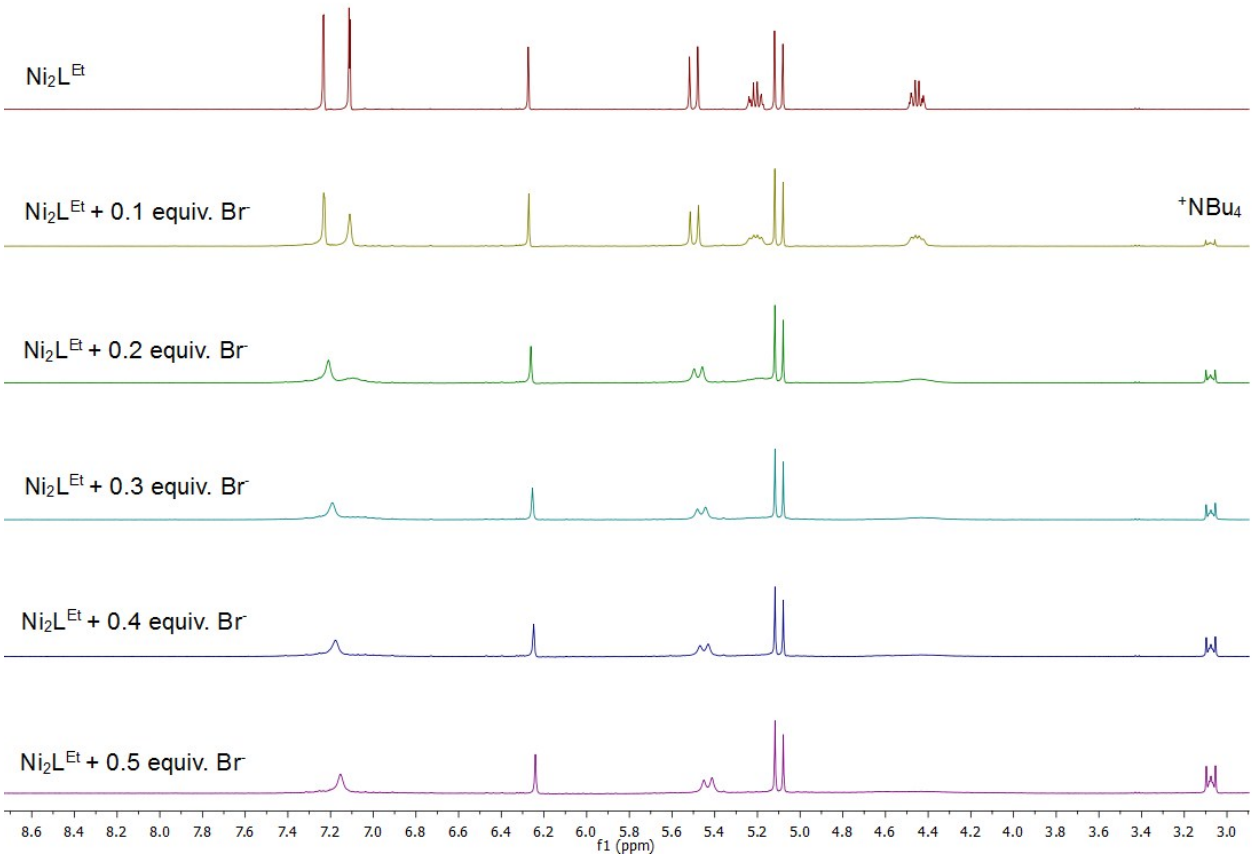

Figure S15: Stacked ^1H NMR spectra of the titration of a solution of NBu_4Br in CD_3CN to a solution of **$Ni_2L^{Et}(PF_6)_2$** in CD_3CN at 400.13 MHz.

7.4 Titration of NBu_4I to **$Ni_2L^{Et}(PF_6)_2$**

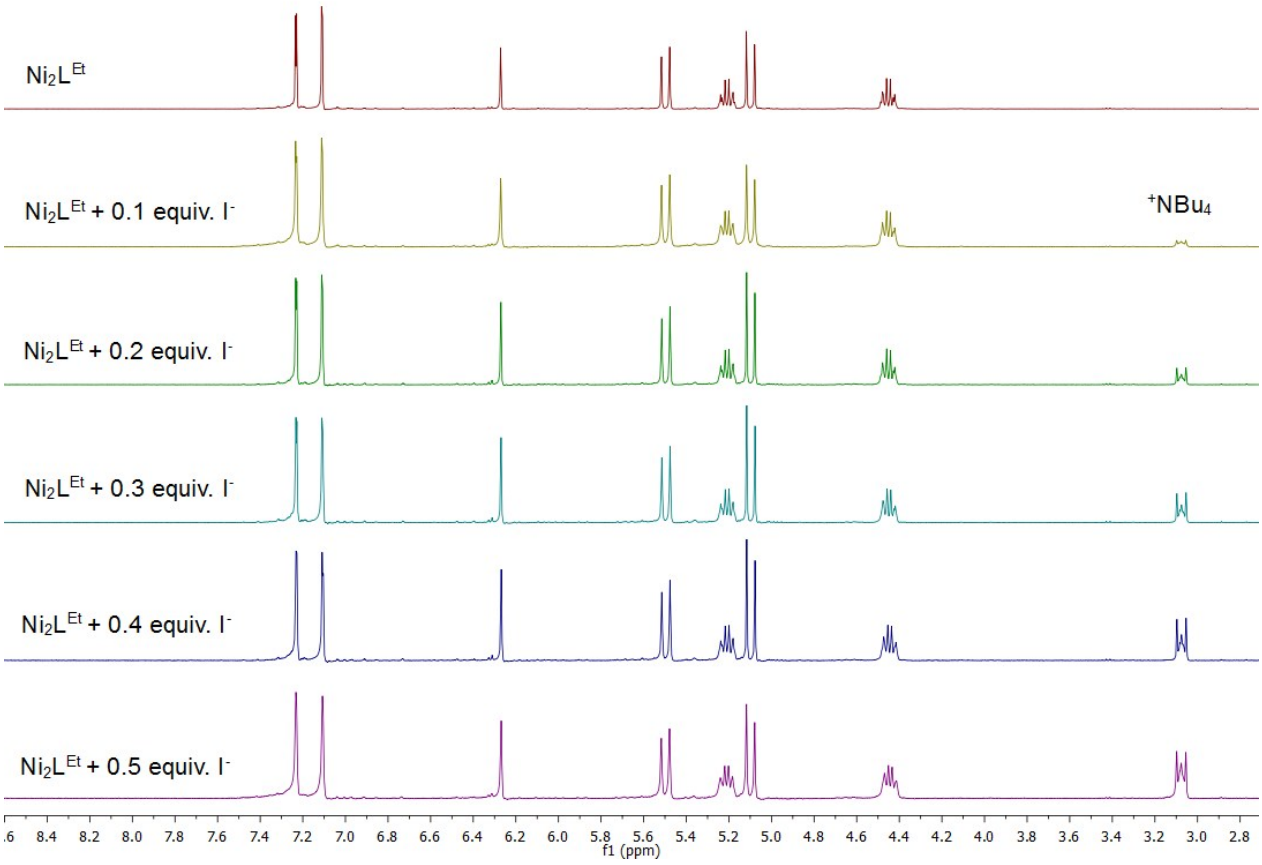

Figure S16: Stacked ^1H NMR spectra of the titration of a solution of NBu_4I in CD_3CN to a solution of **$Ni_2L^{Et}(PF_6)_2$** in CD_3CN at 400.13 MHz.

7.5 Titration of NBu_4Cl to **$[(Ni_2L^{Et})_2Br](PF_6)_3$**

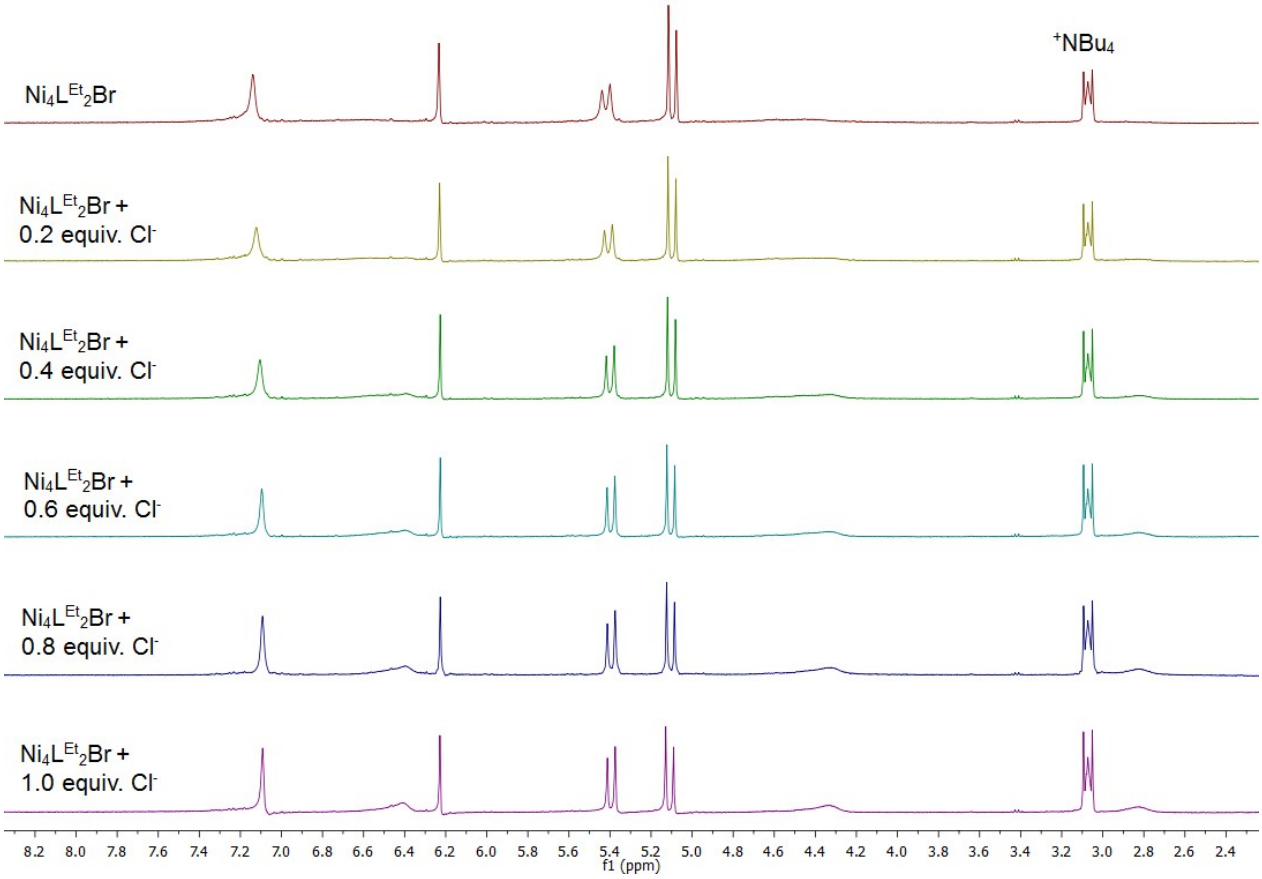

Figure S17: Stacked ^1H NMR spectra of the titration of a solution of NBu_4Cl in CD_3CN to a solution of **$[(Ni_2L^{Et})_2Br](PF_6)_3$** in CD_3CN at 400.13 MHz.

7.6 Titration of NBu_4Br to **$[(Ni_2L^{Et})_2Cl](PF_6)_3$**

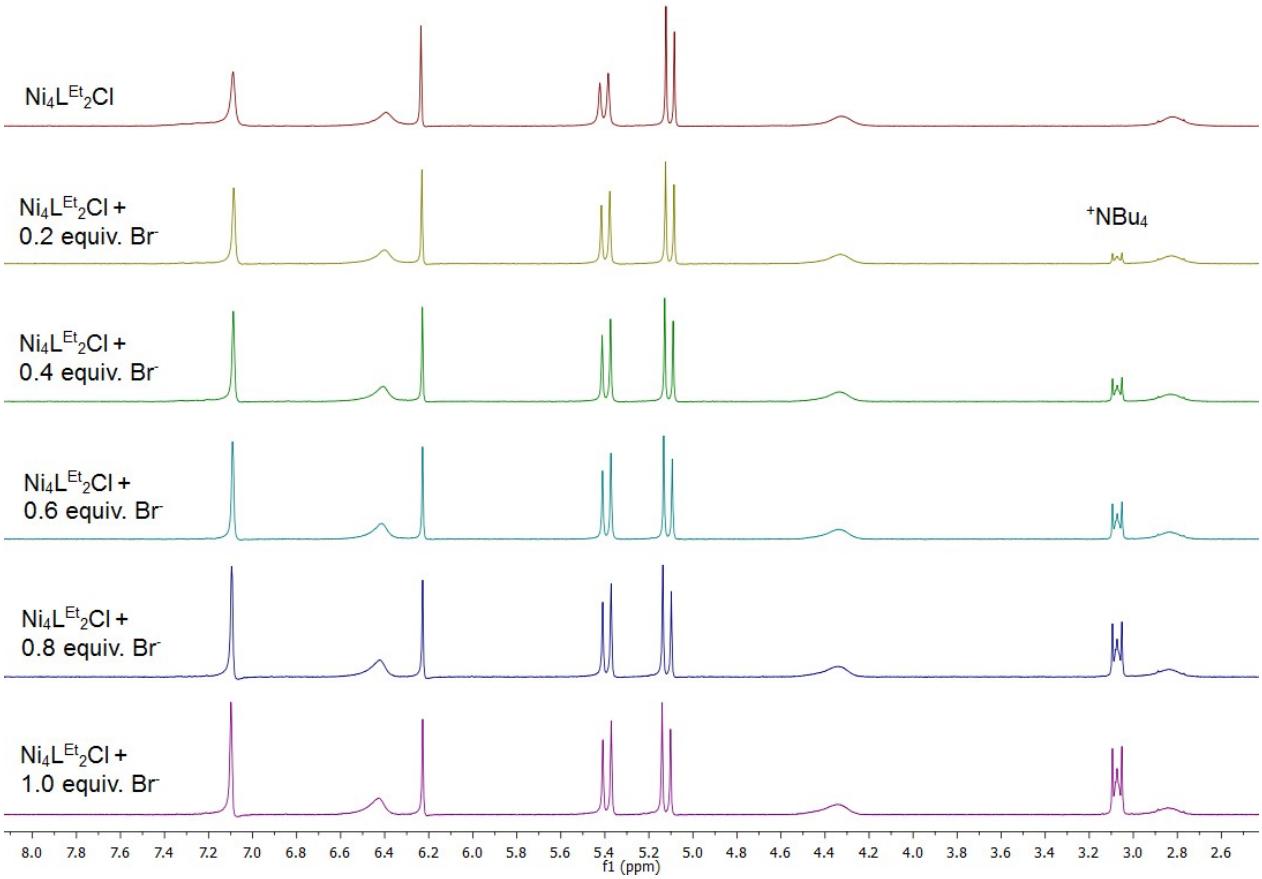

Figure S18: Stacked ^1H NMR spectra of the titration of a solution of NBu_4Br in CD_3CN to a solution of **$[(Ni_2L^{Et})_2Cl](PF_6)_3$** in CD_3CN at 400.13 MHz.

7.7 Titration of NBu_4Cl to **$Ni_2L^{Me}(PF_6)_2$**[2]

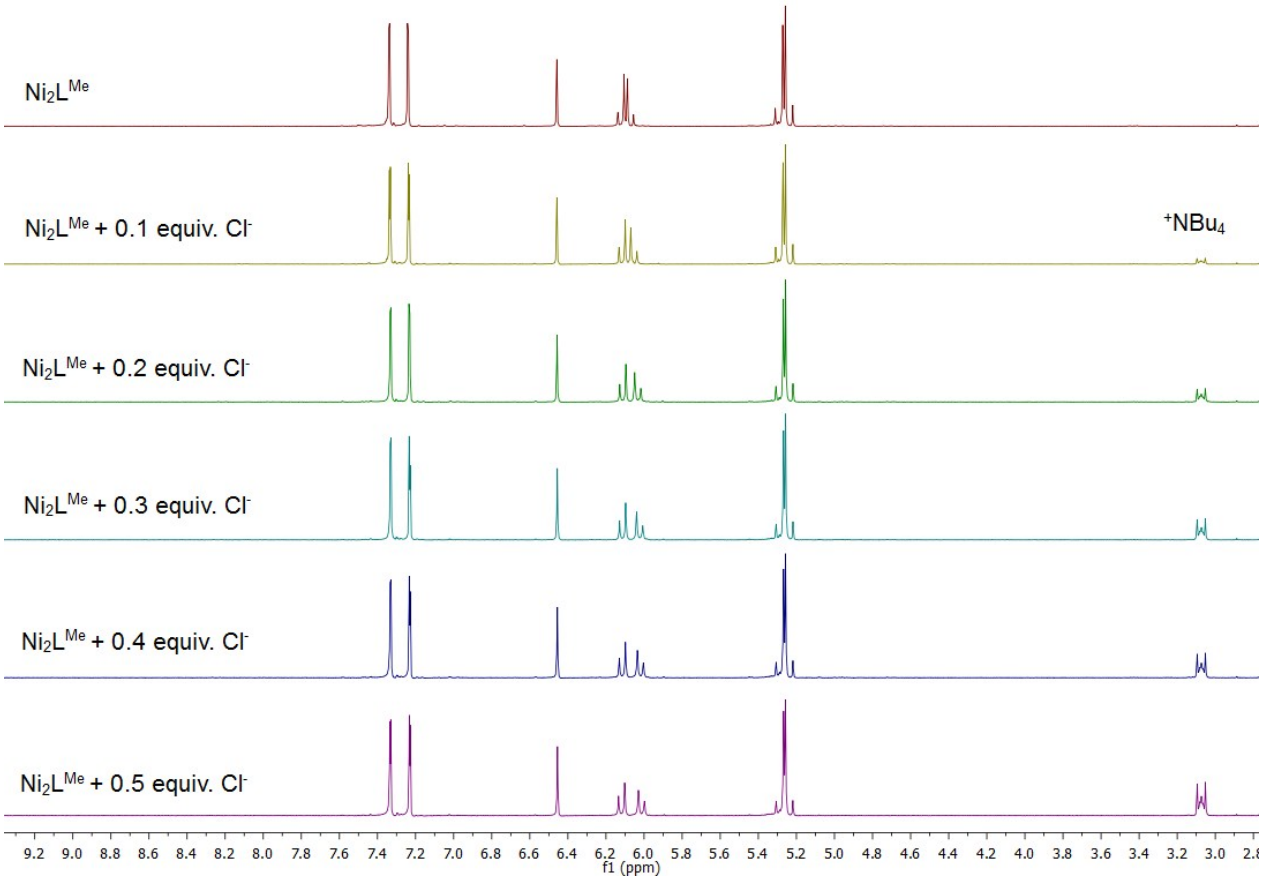

Figure S19: Stacked ^1H NMR spectra of the titration of a solution of NBu_4Cl in CD_3CN to a solution of **$Ni_2L^{Me}(PF_6)_2$** in CD_3CN at 400.13 MHz.

8. Diffusion-Ordered NMR (DOSY) spectra

8.1 $Ni_2L^{Et}(PF_6)_2$

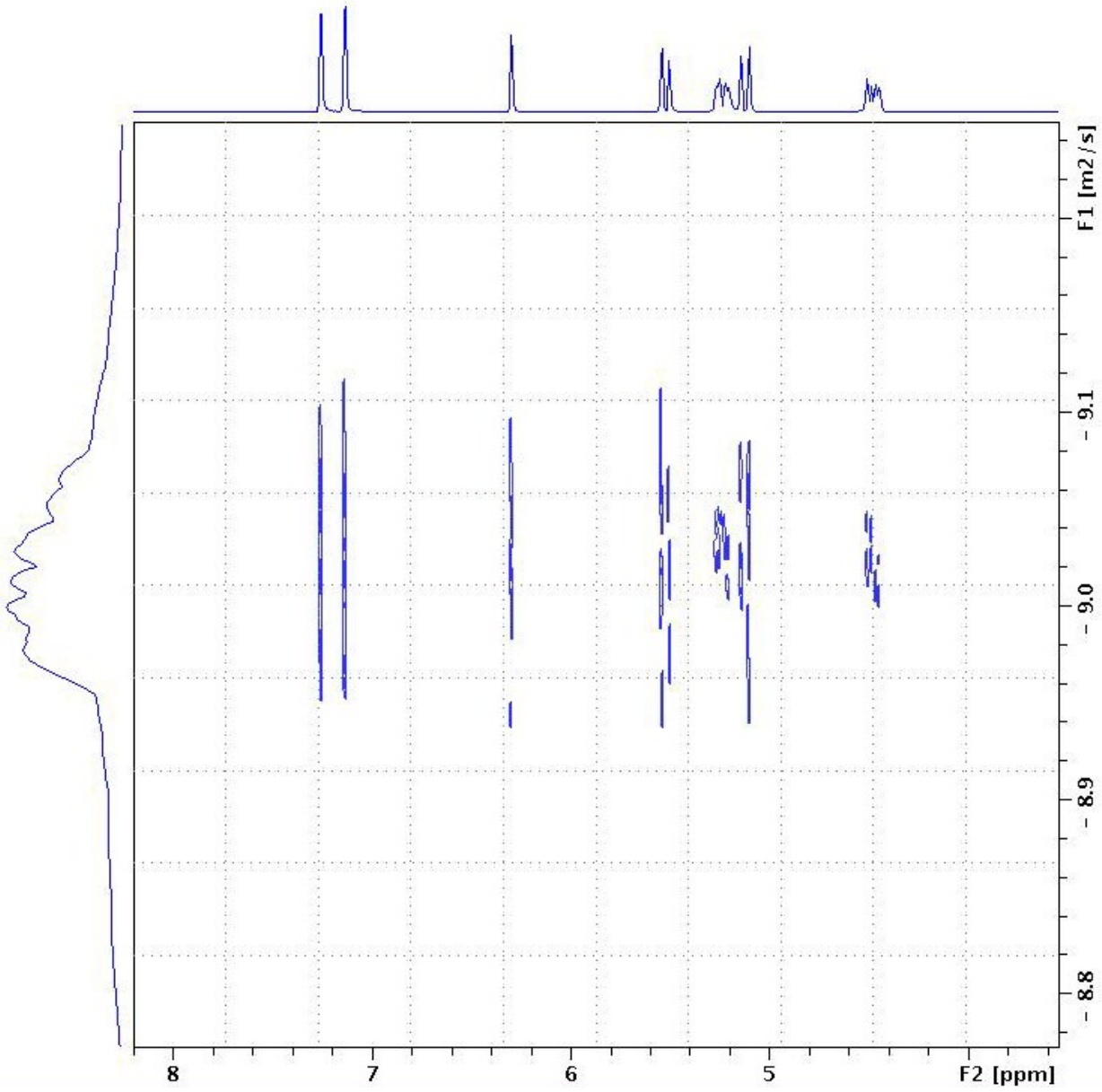

Figure S20: Cutout of the processed 2D DOSY NMR spectrum of $Ni_2L^{Et}(PF_6)_2$.

8.2 **$[(Ni_2L^{Et})_2Cl](PF_6)_3$**

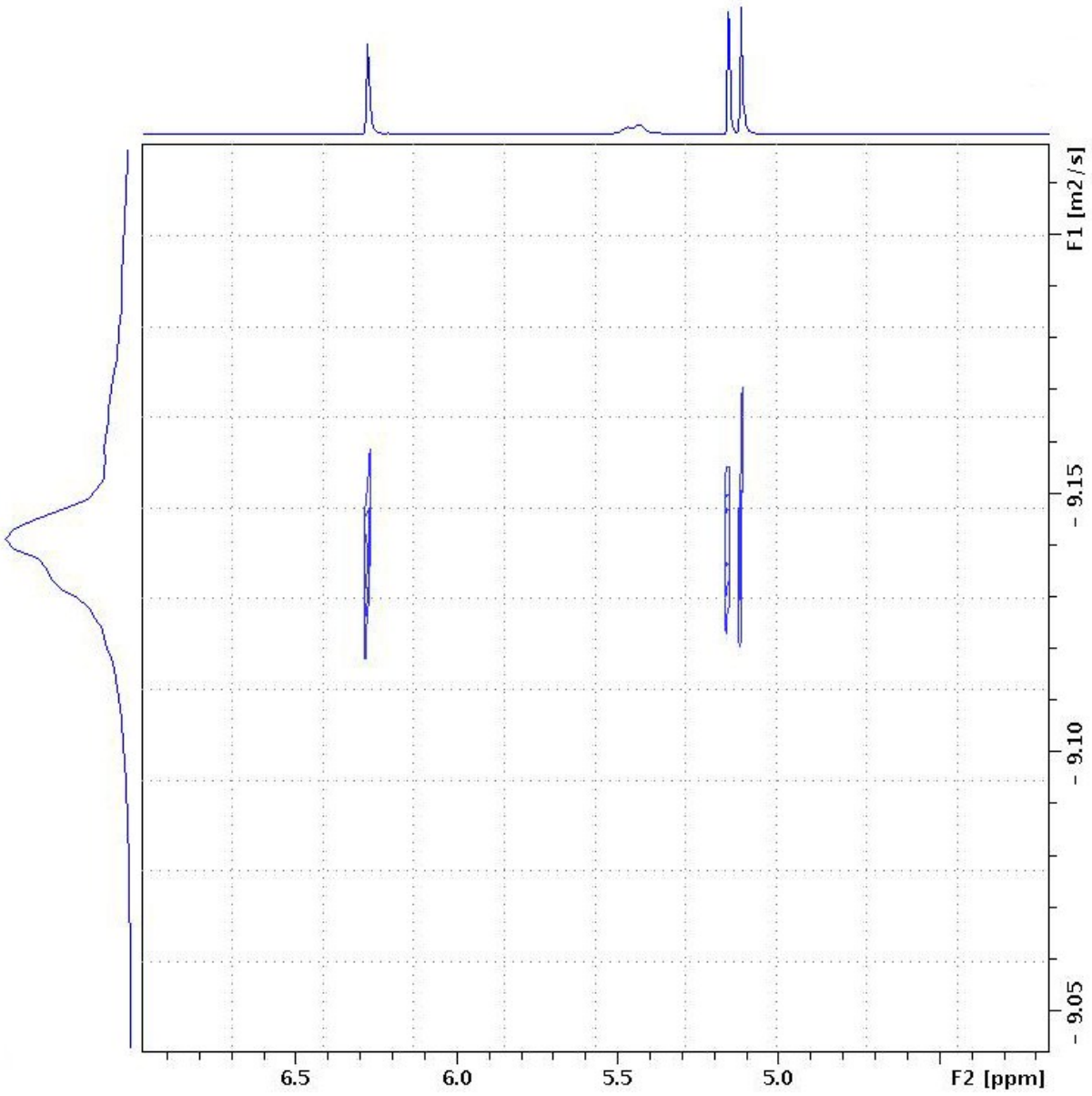

Figure S21: Cutout of the processed 2D DOSY NMR spectrum of **$[(Ni_2L^{Et})_2Cl](PF_6)_3$**.

8.3 **[(Ni$_2$L^{Et})$_2$Br](PF$_6$)$_3$**

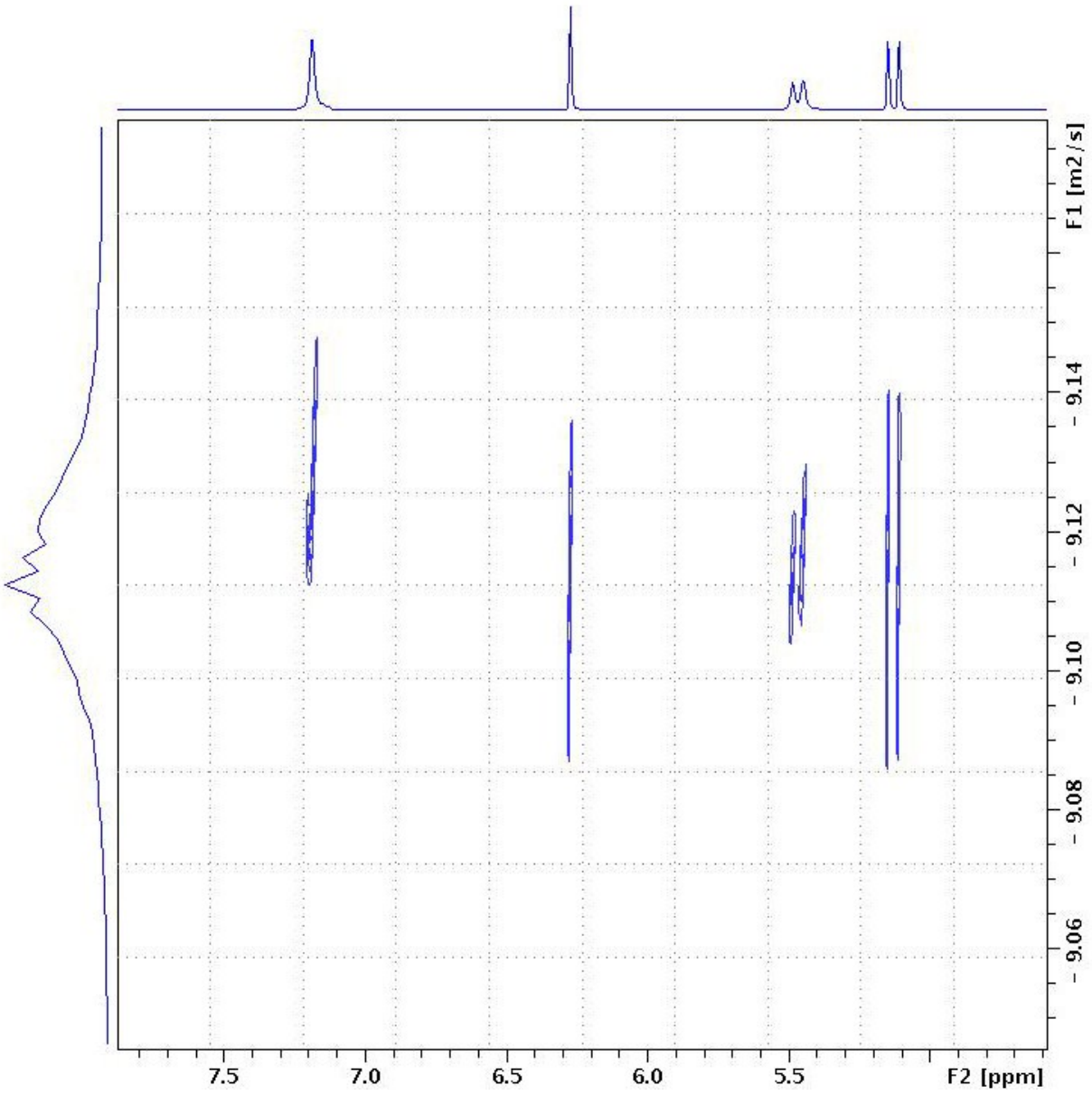

Figure S22: Cutout of the processed 2D DOSY NMR spectrum of **[(Ni$_2$L^{Et})$_2$Br](PF$_6$)$_3$**.

9. Crystallographic details

General:

Data were collected on an X-ray single crystal diffractometer equipped with a CCD detector (APEX II, κ-CCD), a rotating anode (Bruker AXS, FR591) with MoK_α radiation (λ = 0.71073 Å) (Compound **$H_6L^{Et}(PF_6)_4 \cdot MeCN$**) and a graphite monochromator, or a fine-focussed sealed tube and a graphite (compound **$[(Ni_2L^{Et})_2Cl](PF_6)_3$**), or a TRIUMPH monochromator (compounds **$[(Ni_2L^{Et})_2Br](PF_6)_3$**, **$Ni_2L^{Et}(PF_6)_2$**). The APEX II software package was used.[3] The measurements were performed on single crystals coated with perfluorinated ether. The crystals were fixed on the top of a glass fiber and transferred to the diffractometer. Crystals were frozen under a stream of cold nitrogen. A matrix scan was used to determine the initial lattice parameters. Reflections were merged and corrected for Lorenz and polarization effects, scan speed, and background using SAINT.[4] Absorption corrections, including odd and even ordered spherical harmonics were performed using SADABS.[4] Space group assignments were based upon systematic absences, *E* statistics, and successful refinement of the structures. Structures were solved by direct methods with the aid of successive difference Fourier maps, and were refined against all data using the APEX 2 software[3] in conjunction with SHELXL-2014[5] and SHELXLE[6]. Methyl hydrogen atoms were refined as part of rigid rotating groups, with a C–H distance of 0.98 Å and $U_{iso(H)}$ = 1.5·$U_{eq(C)}$. Other H atoms were placed in calculated positions and refined using a riding model, with methylene and aromatic C–H distances of 0.99 and 0.95 Å, respectively, and $U_{iso(H)}$ = 1.2·$U_{eq(C)}$. If not mentioned otherwise, non-hydrogen atoms were refined with anisotropic displacement parameters. Full-matrix least-squares refinements were carried out by minimizing $\Delta w(F_o^2-F_c^2)^2$ with SHELXL-97[7] weighting scheme. Neutral atom scattering factors for all atoms and anomalous dispersion corrections for the non-hydrogen atoms were taken from *International Tables for Crystallography*.[8] Images of the crystal structures were generated by Mercury.[9-12]

Special:

$Ni_2L^{Et}(PF_6)_2$: Geometrical restraints have been applied for disordered solvent molecules and $PF6^-$ anions (see CIF). A residual electron density of approx. 3 eA^{-3} in a distance of 0.64 Å from Ni1 could not be refined accurately due to a not resolvable whole molecule disorder of a small fraction of the entire cationic fragment.

$[(Ni_2L^{Et})_2Cl](PF_6)_3$: Geometrical restraints have been applied for disordered solvent molecules and PF_6^- anions (see CIF).

$[(Ni_2L^{Et})_2Br](PF_6)_3$: Geometrical restraints have been applied for disordered PF_6^- anions (see CIF).

9.1 Compound $\mathbf{H_6L^{Et}(PF_6)_4}$ (CCDC 1448008)

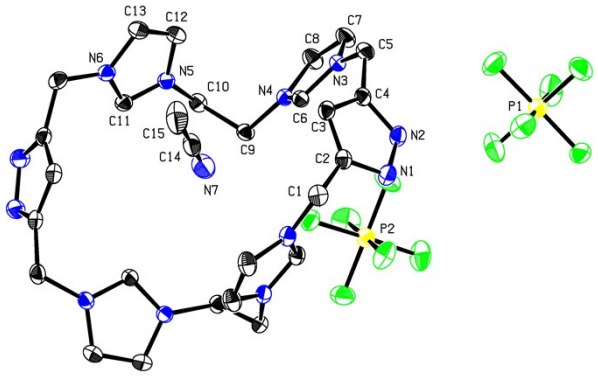

Figure S23: Crystal structure of $\mathbf{H_6L^{Et}(PF_6)_4}\cdot$ **MeCN**. ADPs are given at the 50% probability level.

A clear colourless fragment-like specimen of $C_{14}H_{17.50}F_{12}N_{6.50}P_2$, approximate dimensions 0.081 mm x 0.201 mm x 0.311 mm, was used for the X-ray crystallographic analysis. The X-ray intensity data were measured on a Bruker Kappa APEX II CCD system equipped with a MONTEL mirror monochromator and a Mo FR591 rotating anode (λ = 0.71073 Å).

A total of 4212 frames were collected. The total exposure time was 11.70 hours. The frames were integrated with the Bruker SAINT software package using a narrow-frame algorithm. The integration of the data using a monoclinic unit cell yielded a total of 68857 reflections to a maximum θ angle of 29.13° (0.73 Å resolution), of which 5704 were independent (average redundancy 12.072, completeness = 100.0%, R_{int} = 3.81%, R_{sig} = 1.56%) and 4899 (85.89%) were greater than $2\sigma(F^2)$. The final cell constants of a = 23.2328(16) Å, b =9.5152(6) Å, c = 20.7638(14) Å, β = 112.516(3)°, volume = 4240.2(5) $Å^3$, are based upon the refinement of the XYZ-centroids of 9473 reflections above 20 σ(I) with 4.682° < 2θ <59.26°. Data were corrected for absorption effects using the multi-scan method (SADABS). The ratio of minimum to maximum apparent transmission was 0.910. The calculated minimum and maximum transmission coefficients (based on crystal size) are 0.9050 and 0.9740.
The final anisotropic full-matrix least-squares refinement on F^2 with 314 variables converged at R1 = 4.06%, for the observed data and wR2 = 11.54% for all data. The goodness-of-fit was 1.044. The largest peak in the final difference electron density synthesis was 0.513 $e^-/Å^3$ and the largest hole was -0.324 $e^-/Å^3$ with an RMS deviation of 0.080 $e^-/Å^3$. On the basis of the final model, the calculated density was 1.776 g/cm^3 and F(000), 2280 e^-.

Table S1: Sample and crystal data for $\mathbf{H_6L^{Et}(PF_6)_4}\cdot$ **MeCN**.

Identification code	AltPh27 AP6335-123	
Chemical formula	$C_{14}H_{17.50}F_{12}N_{6.50}P_2$	
Formula weight	566.78	
Temperature	123(2) K	
Wavelength	0.71073 Å	
Crystal size	0.081 x 0.201 x 0.311 mm	
Crystal habit	clear colourless fragment	
Crystal system	monoclinic	
Space group	C 1 2/c 1	
Unit cell dimensions	a = 23.2328(16) Å	α = 90°
	b = 9.5152(6) Å	β = 112.516(3)°
	c = 20.7638(14) Å	γ = 90°
Volume	4240.2(5) $Å^3$	
Z	8	
Density (calculated)	1.776 g/cm^3	
Absorption coefficient	0.328 mm^{-1}	
F(000)	2280	

Table S2: Data collection and structure refinement for $\mathbf{H_6L^{Et}(PF_6)_4}\cdot$ **MeCN**.

Diffractometer	Bruker Kappa APEX II CCD

Radiation source	FR591 rotating anode, Mo
Theta range for data collection	1.90 to 29.13°
Index ranges	-31<=h<=31, -13<=k<=12, -28<=l<=28
Reflections collected	68857
Independent reflections	5704 [R(int) = 0.0381]
Coverage of independent reflections	100.0%
Absorption correction	multi-scan
Max. and min. transmission	0.9740 and 0.9050
Refinement method	Full-matrix least-squares on F^2
Refinement program	SHELXL-2014/6 (Sheldrick, 2014)
Function minimised	$\Sigma\, w(F_o^2 - F_c^2)^2$
Data / restraints / parameters	5704 / 0 / 314
Goodness-of-fit on F^2	1.044
Δ/σ_{max}	0.001
Final R indices	4899 data; I>2σ(I) R1 = 0.0406, wR2 = 0.1081
	all data R1 = 0.0479, wR2 = 0.1154
Weighting scheme	$w=1/[\sigma^2(F_o^2)+(0.0658P)^2+4.6537P]$ where $P=(F_o^2+2F_c^2)/3$
Largest diff. peak and hole	0.513 and -0.324 eÅ^{-3}
R.M.S. deviation from mean	0.080 eÅ^{-3}

9.2 Compound $Ni_2L^{Et}(PF_6)_2$ (CCDC 1448009)

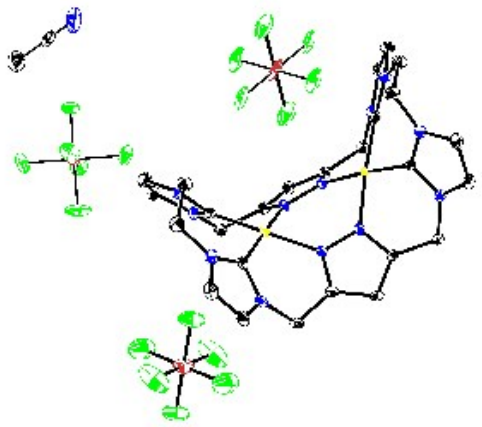

Figure S24: Crystal structure of $Ni_2L^{Et}(PF_6)_2$. ADPs are given at the 50% probability level.

A clear pale yellow fragment-like specimen of $C_{28}H_{29}F_{12}N_{13}Ni_2P_2$, approximate dimensions 0.190 mm x 0.293 mm x 0.449 mm, was used for the X-ray crystallographic analysis. The X-ray intensity data were measured on a Bruker D8 Kappa Apex II system equipped with a Triumph monochromator monochromator and a Mo fine-focus sealed tube (λ = 0.71073 Å).

A total of 4069 frames were collected. The total exposure time was 3.39 hours. The integration of the data using a monoclinic unit cell yielded a total of 164045 reflections to a maximum θ angle of 29.57° (0.72 Å resolution), of which 10093 were independent (average redundancy 16.253, completeness = 100.0%, R_{int} = 4.24%, R_{sig} = 2.10%) and 8365(82.88%) were greater than 2σ(F^2). The final cell constants of a = 15.613(3) Å, b = 13.757(2) Å, c = 16.854(3) Å, β = 96.309(9)°, volume = 3598.1(11) $Å^3$, are based upon the refinement of the XYZ-centroids of 131 reflections above 20 σ(I) with 8.385° < 2θ < 43.45°. The calculated minimum and maximum transmission coefficients (based on crystal size) are 0.6050 and 0.7980.
The final anisotropic full-matrix least-squares refinement on F^2 with 624 variables converged at R1 = 4.30%, for the observed data and wR2 = 11.76% for all data. The goodness-of-fit was 1.072. The largest peak in the final difference electron density synthesis was 2.968 $e^-/Å^3$ and the largest hole was -1.370 $e^-/Å^3$ with an RMS deviation of 0.109 $e^-/Å^3$. On the basis of the final model, the calculated density was 1.763 g/cm^3 and F(000), 1928 e^-.

Table S3: Sample and crystal data for $Ni_2L^{Et}(PF_6)_2$.

Identification code	AltPh43 AP7459-100	
Chemical formula	$C_{28}H_{29}F_{12}N_{13}Ni_2P_2$	
Formula weight	955.00	
Temperature	100(2) K	
Wavelength	0.71073 Å	
Crystal size	0.190 x 0.293 x 0.449 mm	
Crystal habit	clear pale yellow fragment	
Crystal system	monoclinic	
Space group	P 1 21/c 1	
Unit cell dimensions	a = 15.613(3) Å	α = 90°
	b = 13.757(2) Å	β = 96.309(9)°
	c = 16.854(3) Å	γ = 90°
Volume	3598.1(11) $Å^3$	
Z	4	
Density (calculated)	1.763 g/cm^3	
Absorption coefficient	1.242 mm^{-1}	
F(000)	1928	

Table S4: Data collection and structure refinement for $Ni_2L^{Et}(PF_6)_2$.

Diffractometer	Bruker D8 Kappa Apex II
Radiation source	fine-focus sealed tube, Mo
Theta range for data collection	1.92 to 29.57°
Index ranges	-21<=h<=21, -19<=k<=19, -23<=l<=23
Reflections collected	164045
Independent reflections	10093 [R(int) = 0.0424]
Coverage of independent reflections	100.0%
Max. and min. transmission	0.7980 and 0.6050
Refinement method	Full-matrix least-squares on F^2
Refinement program	SHELXL-2014/7 (Sheldrick, 2014)
Function minimised	$\Sigma\ w(F_o^2 - F_c^2)^2$
Data / restraints / parameters	10093 / 202 / 624
Goodness-of-fit on F^2	1.072
Δ/σ_{max}	0.002
Final R indices	8365 data; I>2σ(I) R1 = 0.0430, wR2 = 0.1108
	all data R1 = 0.0542, wR2 = 0.1176
Weighting scheme	$w=1/[\sigma^2(F_o^2)+(0.0524P)^2+7.9515P]$ where $P=(F_o^2+2F_c^2)/3$
Largest diff. peak and hole	2.968 and -1.370 eÅ^{-3}
R.M.S. deviation from mean	0.109 eÅ^{-3}

9.3 Compound $[(Ni_2L^{Et})_2Cl](PF_6)_3$ (CCDC 1448011)

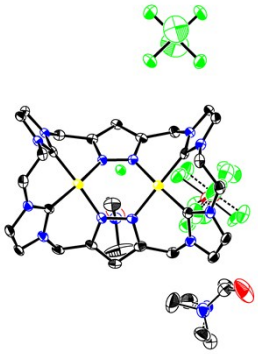

Figure S25: Asymmetric unit of the crystal structure of $[(Ni_2L^{Et})_2Cl](PF_6)_3$. ADPs are given at the 50% probability level.

A clear pale yellow fragment-like specimen of $C_{32}H_{40}Cl_{0.50}F_9N_{14}Ni_2O_2P_{1.50}$, approximate dimensions 0.085 mm x 0.089 mm x 0.432 mm, was used for the X-ray crystallographic analysis. The X-ray intensity data were measured on a Bruker Kappa APEX II CCD system equipped with a graphite monochromator and a Mo fine-focus tube (λ = 0.71073 Å).

A total of 2039 frames were collected. The total exposure time was 33.98 hours. The frames were integrated with the Bruker SAINT software package using a narrow-frame algorithm. The integration of the data using a monoclinic unit cell yielded a total of 36056 reflections to a maximum θ angle of 25.03° (0.84 Å resolution), of which 6903 were independent (average redundancy 5.223, completeness = 99.8%, R_{int} = 9.55%, R_{sig} = 8.59%) and 4585 (66.42%) were greater than $2\sigma(F^2)$. The final cell constants of a = 16.233(3) Å, b =31.342(5) Å, c = 15.432(2) Å, β = 95.632(10)°, volume = 7814.(2) Å^3, are based upon the refinement of the XYZ-centroids of 4698 reflections above 20 σ(I) with 5.198° < 2θ <47.60°. Data were corrected for absorption effects using the multi-scan method (SADABS). The ratio of minimum to maximum apparent transmission was 0.887. The calculated minimum and maximum transmission coefficients (based on crystal size) are 0.6350 and 0.9080.
The structure was solved and refined using the Bruker SHELXTL Software Package in conjunction with SHELXLE, using the space group C 1 2/c 1, with Z = 8 for the formula unit,$C_{32}H_{40}Cl_{0.50}F_9N_{14}Ni_2O_2P_{1.50}$. The final anisotropic full-matrix least-squares refinement on F^2 with 668 variables converged at R1 = 4.53%, for the observed data and wR2 = 9.84% for all data. The goodness-of-fit was 1.010. The largest peak in the final difference electron density synthesis was 0.436 e^-/Å^3 and the largest hole was -0.394 e^-/Å^3 with an RMS deviation of 0.084 e^-/Å^3. On the basis of the final model, the calculated density was 1.709 g/cm^3 and F(000), 4112 e^-.

Table S5: Sample and crystal data for $[(Ni_2L^{Et})_2Cl](PF_6)_3$.

Identification code	AltPh28 AP7337-100	
Chemical formula	$C_{32}H_{40}Cl_{0.50}F_9N_{14}Ni_2O_2P_{1.50}$	
Formula weight	1005.38	
Temperature	100(2) K	
Wavelength	0.71073 Å	
Crystal size	0.085 x 0.089 x 0.432 mm	
Crystal habit	clear pale yellow fragment	
Crystal system	monoclinic	
Space group	C 1 2/c 1	
Unit cell dimensions	a = 16.233(3) Å	α = 90°
	b = 31.342(5) Å	β = 95.632(10)°
	c = 15.432(2) Å	γ = 90°
Volume	7814.(2) Å^3	
Z	8	
Density (calculated)	1.709 g/cm^3	
Absorption coefficient	1.156 mm^{-1}	
F(000)	4112	

Table S6: Data collection and structure refinement for $[(Ni_2L^{Et})_2Cl](PF_6)_3$.

Diffractometer	Bruker Kappa APEX II CCD
Radiation source	fine-focus tube, Mo
Theta range for data collection	2.61 to 25.03°
Index ranges	-19<=h<=19, -37<=k<=37, -18<=l<=18
Reflections collected	36056
Independent reflections	6903 [R(int) = 0.0955]
Coverage of independent reflections	99.8%
Absorption correction	multi-scan
Max. and min. transmission	0.9080 and 0.6350
Structure solution technique	direct methods
Structure solution program	SHELXS-97 (Sheldrick, 2008)
Refinement method	Full-matrix least-squares on F^2
Refinement program	SHELXL-2014/6 (Sheldrick, 2014)
Function minimised	$\Sigma\, w(F_o^2 - F_c^2)^2$
Data / restraints / parameters	6903 / 203 / 668
Goodness-of-fit on F^2	1.010
Δ/σ_{max}	0.001
Final R indices	4585 data; I>2σ(I) R1 = 0.0453, wR2 = 0.0849
	all data R1 = 0.0898, wR2 = 0.0984
Weighting scheme	$w=1/[\sigma^2(F_o^2)+(0.0383P)^2+2.6705P]$ where $P=(F_o^2+2F_c^2)/3$
Largest diff. peak and hole	0.436 and -0.394 eÅ^{-3}
R.M.S. deviation from mean	0.084 eÅ^{-3}

9.4 Compound **$[(Ni_2L^{Et})_2Br](PF_6)_3$** (CCDC 1448010)

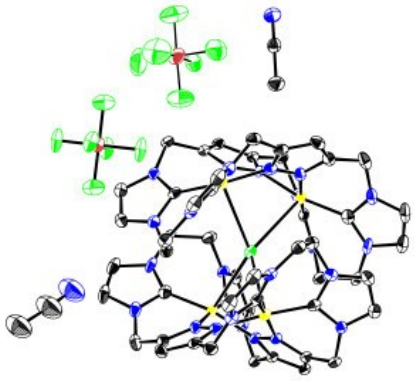

Figure S26: Crystal structure of **$[(Ni_2L^{Et})_2Br](PF_6)_3$**. ADPs are given at the 50% probability level.

A yellow fragment-like specimen of $C_{60}H_{64}BrF_{18}N_{28}Ni_4P_3$, approximate dimensions 0.140 mm x 0.244 mm x 0.300 mm, was used for the X-ray crystallographic analysis. The X-ray intensity data were measured on a Bruker D8 Kappa Apex II system equipped with a Triumph monochromator and a Mo fine-focus sealed tube (λ = 0.71073 Å).

A total of 3528 frames were collected. The total exposure time was 4.90 hours. The frames were integrated with the Bruker SAINT software package using a narrow-frame algorithm. The integration of the data using a monoclinic unit cell yielded a total of 60480 reflections to a maximum θ angle of 25.06° (0.84 Å resolution), of which 6637 were independent (average redundancy 9.113, completeness = 99.6%, R_{int} = 6.49%, R_{sig} = 3.75%) and 5344 (80.52%) were greater than $2\sigma(F^2)$. The final cell constants of a = 15.985(2) Å, b = 30.833(4) Å, c = 15.2616(18) Å, β = 93.494(8)°, volume = 7507.9(15) Å^3, are based upon the refinement of the XYZ-centroids of 95 reflections above 20 σ(I) with 4.097° < 2θ <35.66°. Data were corrected for absorption effects using the multi-scan method (SADABS). The ratio of minimum to maximum apparent transmission was 0.882. The calculated minimum and maximum transmission coefficients (based on crystal size) are 0.6310 and 0.7980.
The final anisotropic full-matrix least-squares refinement on F^2 with 570 variables converged at R1 = 4.43%, for the observed data and wR2 = 11.91% for all data. The goodness-of-fit was 1.106. The largest peak in the final difference electron density synthesis was 0.844 e^-/Å^3 and the largest hole was -1.696 e^-/Å^3 with an RMS deviation of 0.094 e^-/Å^3. On the basis of the final model, the calculated density was 1.705 g/cm^3 and F(000), 3896 e^-.

Table S7: Sample and crystal data for **$[(Ni_2L^{Et})_2Br](PF_6)_3$**.

Identification code	AltPh50 AP7385-100	
Chemical formula	$C_{60}H_{64}BrF_{18}N_{28}Ni_4P_3$	
Formula weight	1927.05	
Temperature	100(2) K	
Wavelength	0.71073 Å	
Crystal size	0.140 mm x 0.244 mm x 0.300 mm	
Crystal habit	yellow fragment	
Crystal system	monoclinic	
Space group	C 1 2/c 1	
Unit cell dimensions	a = 15.985(2) Å	α = 90°
	b = 30.833(4) Å	β = 93.494(8)°
	c = 15.2616(18) Å	γ = 90°
Volume	7507.9(15) Å^3	
Z	4	
Density (calculated)	1.705 g/cm^3	
Absorption coefficient	1.690 mm^{-1}	
F(000)	3896	

Table S8: Data collection and structure refinement for **$[(Ni_2L^{Et})_2Br](PF_6)_3$**.

Diffractometer	Bruker D8 Kappa APEX II

Radiation source	fine-focus sealed tube, Mo
Theta range for data collection	1.91 to 25.06°
Index ranges	-19<=h<=19, -36<=k<=36, -18<=l<=18
Reflections collected	60480
Independent reflections	6637 [R(int) = 0.0649]
Coverage of independent reflections	99.6%
Absorption correction	multi-scan
Max. and min. transmission	0.7980 and 0.6310
Refinement method	Full-matrix least-squares on F^2
Refinement program	SHELXL-2014/7 (Sheldrick, 2014)
Function minimised	$\Sigma\ w(F_o^2 - F_c^2)^2$
Data / restraints / parameters	6637 / 147 / 570
Goodness-of-fit on F^2	1.160
Δ/σ_{max}	0.001
Final R indices	5344 data; I>2σ(I) R1 = 0.0443, wR2 = 0.1099
	all data R1 = 0.0625, wR2 = 0.1191
Weighting scheme	$w=1/[\sigma^2(F_o^2)+(0.0429P)^2+52.9857P]$ where $P=(F_o^2+2F_c^2)/3$
Largest diff. peak and hole	0.844 and -1.696 eÅ^{-3}
R.M.S. deviation from mean	0.094 eÅ^{-3}

10. References

1. E. Lindner, G. von Au and H.-J. Eberle, *Chem. Ber.*, 1981, **114**, 810-813.
2. P. J. Altmann, C. Jandl and A. Pöthig, *Dalton Trans.*, 2015, **44**, 11278-11281.
3. APEX suite of crystallographic software. APEX 2 Version 2008.4. Bruker AXS Inc., Madison, Wisconsin, USA (2008).
4. SAINT, Version 7.56a and SADABS Version 2008/1. Bruker AXS Inc., Madison, Wisconsin, USA (2008).
5. G. M. Sheldrick, "**SHELXL-2014**", University of Göttingen, Göttingen, Germany, (2014).
6. C. B. Huebschle, G. M. Sheldrick and B. Dittrich, "**SHELXLE**", *J. Appl. Cryst.*, 2011, **44**, 1281.
7. G. M. Sheldrick, "**SHELXL-97**", University of Göttingen, Göttingen, Germany, (1998).
8. International Tables for Crystallography, Vol. C, Tables 6.1.1.4 (pp. 500-502), 4.2.6.8 (pp. 219-222), and 4.2.4.2 (pp. 193-199), Wilson, A. J. C., Ed., Kluwer Academic Publishers, Dordrecht, The Netherlands, 1992.
9. C. F. Macrae, I. J. Bruno, J. A. Chisholm, P. R. Edgington, P. McCabe, E. Pidcock, L. Rodriguez-Monge, R. Taylor, J. van de Streek and P. A. Wood, *J. Appl. Crystallogr.*, 2008, **41**, 466-470.
10. C. F. Macrae, P. R. Edgington, P. McCabe, E. Pidcock, G. P. Shields, R. Taylor, M. Towler and J. Van de Streek, *J. Appl. Crystallogr.*, 2006, **39**, 453-457.
11. I. J. Bruno, J. C. Cole, P. R. Edgington, M. K. Kessler, C. F. Macrae, P. McCabe, J. Pearson and R. Taylor, *Acta Cryst.*, 2002, **B58**, 389-397.
12. R. Taylor and C. F. Macrae, *Acta Cryst.*, 2001, **B57**, 815-827.